

Geology of the Waterford Quadrangle, Virginia and  
Maryland, and the Virginia Part of the  
Point of Rocks Quadrangle

U.S. GEOLOGICAL SURVEY BULLETIN 2095





# Geology of the Waterford Quadrangle, Virginia and Maryland, and the Virginia Part of the Point of Rocks Quadrangle

By William C. Burton, Albert J. Froelich, John S. Pomeroy, and K.Y. Lee

---

U.S. GEOLOGICAL SURVEY BULLETIN 2095

*A detailed study of the surficial and bedrock geology of part of the Blue Ridge province and Culpeper basin in northern Virginia and Maryland*



UNITED STATES GOVERNMENT PRINTING OFFICE, WASHINGTON : 1995

**U.S. DEPARTMENT OF THE INTERIOR**  
**BRUCE BABBITT, Secretary**

**U.S. GEOLOGICAL SURVEY**  
**GORDON P. EATON, Director**

For sale by U.S. Geological Survey, Information Services  
Box 25286, Federal Center, Denver, CO 80225

Any use of trade, product, or firm names in this publication is for descriptive purposes only and does not imply endorsement by the U.S. Government.

Published in the Eastern Region, Reston, Va.  
Manuscript approved for publication April 29, 1994.

**Library of Congress Cataloging in Publication Data**

Geology of the Waterford quadrangle, Virginia and Maryland, and the Virginia part of the Point of Rocks quadrangle / by William C. Burton...[et al.].

p. cm. — (U.S. Geological Survey bulletin ; 2095)

Includes bibliographical references.

Supt. of Docs. no.: I 19.3:2095

1. Geology—Virginia. 2. Geology—Maryland. I. Burton, William C. (William Chapin), 1952–. II. Series.

QE75.B9 no. 2095

[QE173]

557.3 s—dc20

[557.55]

94-20824  
CIP

# CONTENTS

|  |    |
|--|----|
| Abstract.....  | 1  |
| Introduction.....  | 2  |
| Geology of Proterozoic and Paleozoic Rocks.....                      | 2  |
| Middle Proterozoic Basement.....                                     | 2  |
| Granitic Gneiss.....   | 3  |
| U-Pb Ages of Granitic Gneisses.....                                  | 5  |
| Layered and Mafic Gneisses.....                                      | 5  |
| Middle Proterozoic Fabric and Structures.....                        | 7  |
| Middle Proterozoic Metamorphism.....                                 | 7  |
| Late Proterozoic Dikes.....  | 8  |
| Dike Lithology.....  | 8  |
| Dike Density and Orientations.....                                   | 8  |
| Geochemistry.....  | 9  |
| U-Pb Age of Rhyolite Dike.....                                       | 11 |
| Late Proterozoic Metasedimentary and Metavolcanic Rocks.....         | 12 |
| Swift Run Formation.....   | 12 |
| Catoctin Formation.....  | 13 |
| Possible Rift-Related Faults.....                                    | 14 |
| Chilhowee Group Metasedimentary Rocks.....                           | 15 |
| Loudoun Formation.....   | 15 |
| Weverton Quartzite.....  | 15 |
| Harpers Formation.....   | 16 |
| Antietam Quartzite.....  | 16 |
| Post-Chilhowee Group Metasedimentary Rocks.....                      | 16 |
| Carbonaceous Phyllite.....   | 16 |
| Tomstown Dolomite and Frederick Limestone.....                       | 17 |
| Paleozoic Structure and Metamorphism.....                            | 17 |
| First-Generation Paleozoic Cleavage.....                             | 17 |
| First-Generation Folds.....  | 19 |
| Second-Generation Cleavage and Folds.....                            | 19 |
| Late Folds.....  | 19 |
| The Tectonic Role of Faulting.....                                   | 20 |
| Late Brittle Structures.....   | 20 |
| Paleozoic Recrystallization and Metamorphic Grade.....               | 21 |
| <sup>40</sup> Ar/ <sup>39</sup> Ar Dating of Metamorphic Fabric..... | 22 |
| Geology of Early Mesozoic Rocks.....                                 | 22 |
| Sedimentary Rocks.....   | 22 |
| Manassas Sandstone, Poolesville Member.....                          | 22 |
| Balls Bluff Siltstone and its Leesburg Member.....                   | 23 |
| Igneous and Metamorphic Rocks.....                                   | 24 |
| Diabase.....   | 24 |
| Thermally Metamorphosed Rocks.....                                   | 25 |
| Structural Geology.....  | 25 |
| Bull Run Fault.....  | 25 |
| Furnace Mountain Fault and Related Faults and Lineament.....         | 25 |
| Inferred Faults.....   | 26 |
| Relative Timing of Mesozoic Faulting.....                            | 26 |
| Joints in the Culpeper Basin.....                                    | 26 |
| Surficial Geology.....   | 26 |
| Economic Geology.....  | 27 |
| Hydrogeology.....  | 27 |
| References Cited.....  | 28 |

## PLATE

[Plate is in pocket]

1. Geologic map of the Waterford quadrangle, Virginia and Maryland, and the Virginia part of the Point of Rocks quadrangle.

## FIGURES

1. Map showing the study area, and mapping coverage by authors, of the Waterford quadrangle, Virginia and Maryland, and the Virginia part of the Point of Rocks quadrangle ..... 3
2. Lower hemisphere equal-area projections of structures of Middle Proterozoic age..... 5
3. Photomicrograph showing thin section of garnet graphite paragneiss, Waterford quadrangle..... 6
4. Photomicrograph showing thin section of hornblende metanorite, Waterford quadrangle ..... 6
5. Diagrams showing orientation of Late Proterozoic dikes ..... 9
6. AFM diagram showing Late Proterozoic metadiabase and metabasalt ..... 9
7. Variation diagrams of Late Proterozoic metadiabase and metabasalt..... 12
8. Chondrite-normalized REE diagram of Late Proterozoic metadiabase and metabasalt ..... 12
9. Photograph showing recumbent, isoclinal  $F_1$  folds and more open, upright  $F_2$  folds with associated steeply dipping crenulation cleavage in interlayered phyllite and quartzite of the Loudoun Formation ..... 15
10. Photograph of outcrop on western flank of Catoctin Mountain, just east of Furnace Mountain, showing upright, post- $F_2$  kink folds in  $S_1$ -laminated quartzose phyllite of the Harpers Formation ..... 16
11. Photomicrograph showing thin section of well-developed  $S_1$  in quartzose phyllite of the Harpers Formation, Point of Rocks quadrangle ..... 16
- 12–15. Lower hemisphere equal-area projections of—
  12. First- and second-generation structures of Paleozoic age ..... 18
  13. Late folds..... 20
  14. Late brittle structures in pre-Mesozoic rocks ..... 21
  15. Contoured poles to joints in the Culpeper basin ..... 21
16. Photograph showing outcrop of carbonate conglomerate, Leesburg Member of Balls Bluff Siltstone, just west of junction of State Routes 661 and 15..... 23

## TABLES

1. Mineral compositions in volume percent of samples of five Middle Proterozoic rock units..... 4
2. Major oxide and trace-element geochemistry of four Middle Proterozoic rocks..... 4
3. Major oxide and trace-element abundances and averages of Late Proterozoic metadiabase, metabasalt, and metarhyolite ..... 10
4. Major oxide geochemistry of high-titanium, quartz-normative Jurassic diabase dike, Waterford quadrangle..... 24

## METRIC CONVERSION FACTORS

| Multiply        | By            | To obtain |
|-----------------|---------------|-----------|
|                 | <i>Length</i> |           |
| millimeter (mm) | 0.03937       | inch      |
| centimeter (cm) | 0.3937        | inch      |
| decimeter (dm)  | 3.937         | inch      |
| meter (m)       | 3.281         | foot      |
| kilometer (km)  | 0.6214        | mile      |

# Geology of the Waterford Quadrangle, Virginia and Maryland, and the Virginia Part of the Point of Rocks Quadrangle

By William C. Burton, Albert J. Froelich<sup>1</sup>, John S. Pomeroy, and K.Y. Lee<sup>1</sup>

## ABSTRACT

The bedrock geology of the Waterford quadrangle and of the Virginia part of the Point of Rocks quadrangle consists of a portion of the Middle Proterozoic basement core and its cover sequence on the eastern limb of the Blue Ridge anticlinorium and the adjacent early Mesozoic Culpeper basin. The three major rock associations in this area are (1) Middle Proterozoic gneisses, which have been extensively intruded by Late Proterozoic metadiabase dikes, (2) unconformably overlying Late Proterozoic and early Paleozoic metavolcanic and metasedimentary rocks, and (3) Upper Triassic sedimentary strata intruded by Early Jurassic diabase. The Triassic and Jurassic rocks are separated from the older rocks of the anticlinorium to the west by a major normal fault, the Bull Run fault. Late Cenozoic surficial deposits of three major types unconformably overlie the bedrock: colluvium derived from Catoctin Mountain, terrace deposits of the Potomac River, and flood plain alluvium of the Potomac River and its tributaries.

The Middle Proterozoic rocks of the core of the anticlinorium consist of four types of granitic orthogneiss as well as a suite of nongranitic rocks that occur in discontinuous lenses and are inferred to predate the orthogneisses. All of the gneisses contain high-grade metamorphic assemblages and structures of probable Middle Proterozoic (Grenvillian) age (~1 Ga), with both northeast- and northwest-trending foliations and a southeast-plunging mineral lineation. Intruding these rocks are northeast-striking dikes of metadiabase, which locally constitute more than 50 percent of the bedrock, and rare metarhyolite. The metadiabase dikes resemble in bulk composition the overlying Catoctin Formation metabasalts for which they were probably feeders.

Nonconformably overlying the gneiss-dike complex is a sequence of variegated clastic metasedimentary and metavolcanic rocks of the Swift Run and Catoctin Formations. The Catoctin is overlain by metamorphosed clastic rocks of the Chilhowee Group, which consists of the Loudoun Formation, Weverton Quartzite, Harpers Formation, and Antietam Quartzite. Locally overlying the Chilhowee

metasediments is a thin, discontinuous, carbonaceous phyllite that grades laterally into and is overlain by Tomstown Dolomite, which is in turn overlain by the Frederick Limestone. The Loudoun Formation and the rocks above the Chilhowee Group are limited to the northern part of the map area.

All of the rocks of the Blue Ridge anticlinorium were strongly deformed and subjected to greenschist-facies metamorphism, probably in the late Paleozoic. The deformation produced a penetrative, well-developed northeast-striking schistosity and a later spaced cleavage, each accompanied by an episode of folding. The older episode of folding, and formation of the penetrative schistosity, is probably associated with the formation of the anticlinorium, whereas the second phase is well developed only on the eastern limb, particularly at the northern end of Catoctin Mountain in Virginia. Several later, minor fold phases also occur in this region. Metamorphism associated with the Paleozoic deformation reached biotite grade and produced retrograde micaeous mineral assemblages in the basement gneisses, greenschist-facies minerals in the metadiabase dikes and metabasalts of the Catoctin Formation, and prograde muscovite and biotite in the clastic metasediments. Muscovite in the cover-sequence metasedimentary rocks that grew during formation of the Paleozoic schistosity has been dated by the <sup>40</sup>Ar/<sup>39</sup>Ar age-spectrum technique as probable late Paleozoic.

The regionally deformed and metamorphosed Proterozoic and Paleozoic rocks of the Blue Ridge anticlinorium in the west are separated from the early Mesozoic rocks of the Culpeper basin in the eastern part of the map area by the north-striking, east-dipping Bull Run normal fault, which has a throw of thousands of meters. The Upper Triassic sedimentary rocks of the basin consist of three major units: (1) red sandstone and siltstone (Poolesville Member of the Manassas Sandstone), which is overlain by (2) red siltstone, sandstone, and shale (Balls Bluff Siltstone) that laterally interfingers with (3) carbonate conglomerate (Leesburg Member of the Balls Bluff Siltstone). These sedimentary rocks are locally intruded by Early Jurassic diabase, which also intrudes rocks of the anticlinorium to the west. The Triassic sedimentary rocks are gently warped and mostly west dipping, are truncated on the west by the Bull Run fault, and

---

<sup>1</sup>Deceased.

are inferred to be cut by a number of unexposed cross-basin normal faults.

The map area contains three types of surficial deposits of late Cenozoic age. Colluvium largely derived from Catoctin Mountain blankets both the uplands of the Blue Ridge anticlinorium and the lowlands of the Culpeper basin. Quaternary terrace deposits of the Potomac River occur as isolated patches on the Triassic rocks of the Culpeper basin. Alluvium occurs in both the Potomac River flood plains and the streambeds of its tributaries. Features associated with ground-water recharge and discharge, respectively, in the Culpeper basin include sinkholes and depressions, springs, and tufa deposits.

## INTRODUCTION

*Geologic Setting.*—The map area of this report (pl. 1, in pocket) includes a portion of the eastern limb of the Blue Ridge anticlinorium and a portion of the western part of the Culpeper basin south of the Potomac River in Virginia and east of the Potomac in Maryland. From west to east the bedrock consists of rocks of the basement core of the anticlinorium, including Middle Proterozoic gneisses that are cut by a sheeted dike complex of Late Proterozoic age; a generally east dipping sequence of Late Proterozoic to Cambrian low-grade metasedimentary and metavolcanic rocks that rests unconformably on basement; a moderately east dipping normal fault and associated faults of early Mesozoic age; and generally west dipping sedimentary rocks cut by minor intrusive diabase in the early Mesozoic Culpeper basin. These rocks bear evidence of four major tectonic events: the ~1-Ga Grenville orogeny, the ~600-Ma Iapetan rifting event, the ~300-Ma Alleghany orogeny, and the ~200-Ma early Mesozoic rifting event. Physiographically the rifted basement core of the anticlinorium and the Culpeper basin occupy a subdued plateau and lowlands, respectively, whereas the deformed metasedimentary and metavolcanic rocks underlie the north-trending ridge of Catoctin Mountain and its flanking uplands.

*Previous Work in the Map Area.*—This area has been mapped at smaller scales by several previous authors. Keith (1894), Jonas and Stose (1938), and Stose and Stose (1946) mapped a large area of the Blue Ridge in Maryland and Virginia, characterizing the local stratigraphy and general style of Appalachian deformation. Cloos (1941, 1947), in his mapping in Maryland, developed the concept of a large west-verging anticlinorium that is cored by basement; the Catoctin Mountain represents the eastern, upright limb. Whittaker (1955) mapped Catoctin Mountain from Leesburg north to its termination near Emmitsburg, Md. Nunan (1979) studied the stratigraphy of the Weverton Formation in an area that included Catoctin Mountain. Howard (1991) did a reconnaissance of Blue Ridge basement lithologies that included some rocks in the map area. Previous studies

of the Culpeper basin that include the present map area include Lee (1977, 1979), Lee and Froelich (1989), Froelich and others (1982), and Lindholm (1979).

*New Work in the Map Area.*—Contributions made by this report include detailed mapping of the basement core of the Blue Ridge anticlinorium, including delineation of individual Iapetan-stage dikes and previously unrecognized units in the Middle Proterozoic gneisses; mapping of a number of stratigraphic units in the lower cover-sequence metasedimentary and metavolcanic rocks (Fauquier and Catoctin Formations); a refined interpretation of the structures on the eastern limb of the Blue Ridge anticlinorium; and detailed mapping of units and interpretation of block faulting in the early Mesozoic Culpeper basin. Isotopic ages obtained from various units in this study include U-Pb dating of zircons from a Late Proterozoic metarhyolite dike (Aleinikoff and others, 1995) and Middle Proterozoic granite gneiss (Aleinikoff and others, 1993) and  $^{40}\text{Ar}/^{39}\text{Ar}$  ages from cleavage-defining muscovite associated with Paleozoic structures in the cover-sequence rocks (Burton and others, 1992a).

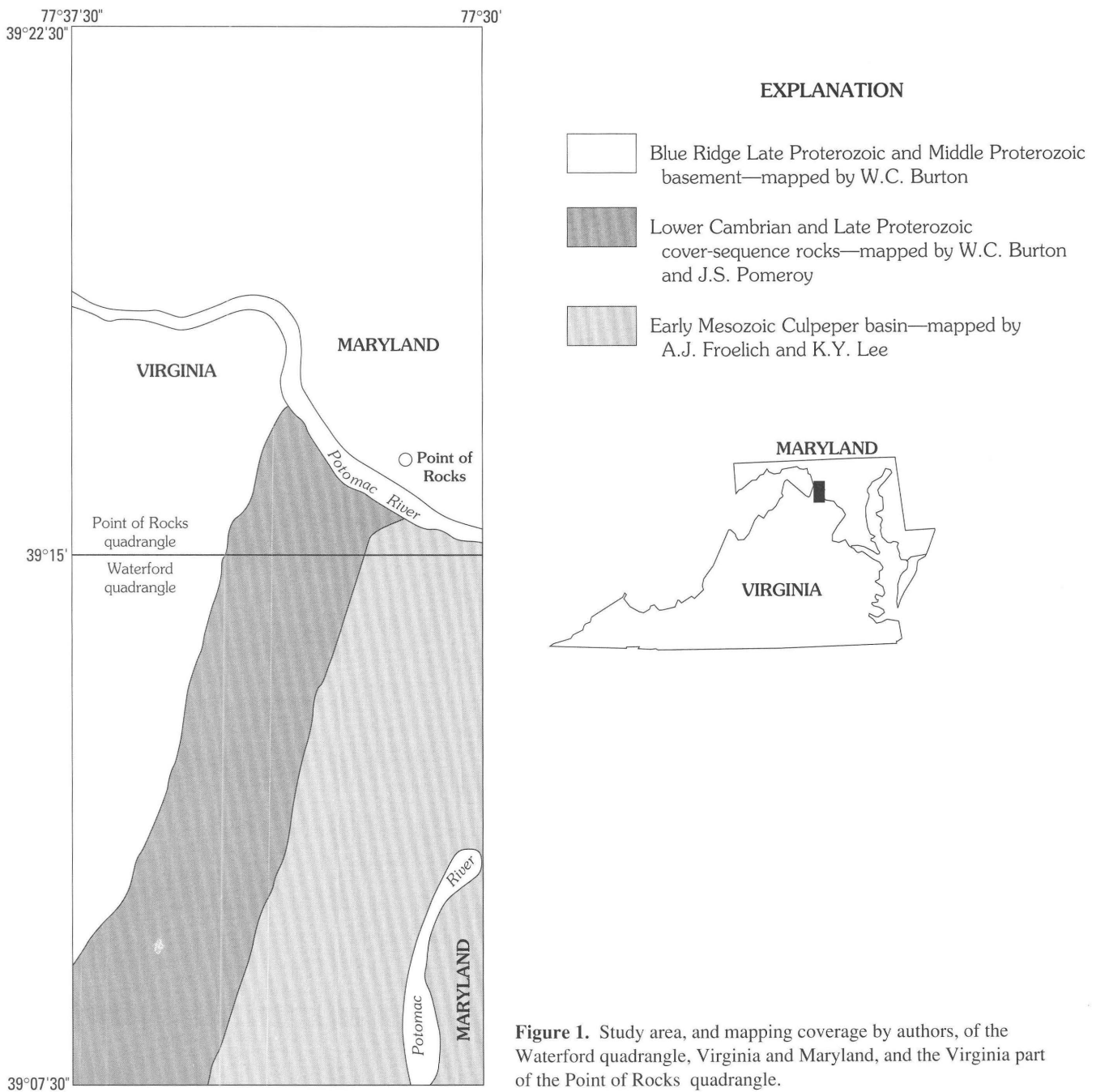
*Map Coverage.*—This map and report combines the work of four geologists (fig. 1). Burton mapped the basement and most of the cover-sequence rocks west of the Culpeper basin at an original scale of 1:12,000, by using base maps provided by the Loudoun County Department of Natural Resources. The data were compiled later on U.S. Geological Survey 1:24,000 topographic base maps. Pomeroy mapped some of the cover rocks at 1:12,000 and compiled the data at 1:24,000. Lee did much of the original mapping of the Culpeper basin in the map area at 1:24,000 (Lee, 1979), and his work was revised by Froelich. The final compilation (pl. 1) and most of the text and figures are by Burton.

*Acknowledgments.*—The authors gratefully acknowledge the support of the Loudoun County Department of Natural Resources, which provided funding for mapping and research, 1:12,000-scale base maps, and other information used in this report. Peter T. Lyttle (U.S. Geological Survey) provided previously unpublished geochemical data.

## GEOLOGY OF PROTEROZOIC AND PALEOZOIC ROCKS

### MIDDLE PROTEROZOIC BASEMENT

The basement core of the Blue Ridge anticlinorium exposed in the map area (pl. 1) contains Middle Proterozoic gneisses, and younger, crosscutting Late Proterozoic igneous dikes. The Middle Proterozoic gneisses include two main types: relatively homogeneous granitic orthogneisses and variegated, well-foliated or layered metasedimentary and metaigneous gneisses of nongranitic composition. Granite gneiss is volumetrically the most abundant and encloses discontinuous belts and lenses of nongranitic



layered and mafic gneiss. The bodies of layered and mafic gneiss may represent remnants of a previous sedimentary-volcanic terrane that was subjected to widespread intrusion and (or) partial melting during or before the ~1-Ga Middle Proterozoic (Grenvillian) high-grade metamorphic event (Burton and Southworth, 1993). All of the gneisses contain recognizable Middle Proterozoic fabrics and structural trends that have been variably overprinted by Paleozoic deformation.

#### GRANITIC GNEISS

Four granitic gneiss units have been mapped in this area: relatively biotite-rich granite gneiss (Y<sub>bgg</sub>), biotite-poor leucocratic granite gneiss (Y<sub>gg</sub>), garnet-bearing leucocratic granite gneiss (Y<sub>gt</sub>), and biotitic Marshall Metagranite (Y<sub>mb</sub>). The recognition of biotite-poor granite gneiss, biotite-rich granite gneiss, and garnetiferous granite gneiss parallels Howard's (1991) facies A, B, and C, respectively.

**Table 1.** Mineral compositions in volume percent of samples of five Middle Proterozoic rock units, based on point counts in thin section (one thin section per sample).

[—, not found]

| Mineral   | Map unit<br>Description<br>(sample number)         |  |  |  |  |
|---|--|--|--|--|--|
|   | Ygg<br>Leucocratic<br>granite<br>gneiss<br>(BR-11) | Ybgg<br>Biotite<br>granite<br>gneiss<br>(BR-554) | Yqp<br>Quartz-<br>plagioclase<br>gneiss<br>(BR-36) | Yrg<br>Rusty<br>paragneiss<br>(BR-595) | Yhp<br>Hornblende<br>metanorite<br>(BR-602A) |
| Quartz  | 35   | 33   | 24   | 30                                     | —  |
| Plagioclase                                     | 22   | 23   | 45   | 43                                     | 58   |
| Microcline (or<br>perthite).                    | 39   | 19   | —  | —                                      | —  |
| Biotite   | 3  | 14   | 14   | 1                                      | —  |
| Garnet  | —  | —  | —  | 5                                      | —  |
| Graphite  | —  | —  | —  | 3                                      | —  |
| Orthopyroxene                                   | —  | —  | —  | —                                      | 35   |
| Hornblende                                      | —  | —  | —  | —                                      | 5  |
| Ilmenite/sphene                                 | <1   | <1   | 2  | —                                      | 1  |
| Apatite   | —  | —  | <1   | —                                      | <1   |
| Chlorite (from<br>garnet).                      | —  | —  | —  | 15                                     | —  |
| Clinozoisite/<br>epidote (from<br>plagioclase). | —  | 2  | 7  | 1                                      | 1  |
| Muscovite (from<br>plagioclase).                | <1   | 8  | 8  | <1                                     | —  |
| Rutile  | —  | —  | —  | 2                                      | —  |
| Total counts<br>per sample.                     | 592  | 556  | 571  | 537                                    | 508  |

Modes for the first two units (Ybgg and Ygg) are shown in table 1, and major oxide and trace-element geochemistry of single samples of both units is shown in table 2. In these units the Grenville metamorphic texture is characterized in thin section by a flattened granoblastic-elongate fabric defined by aligned flakes of biotite and flattened grains of quartz, plagioclase, and microcline. The microcline commonly has subordinate amounts of perthite. The biotite-rich gneiss (Ybgg) is commonly well foliated and weathers to a reddish-orange color, which locally has a rusty tint due to disseminated magnetite. The leucocratic gneiss (Ygg) typically weathers white to light gray and has little or no biotite. A weak Middle Proterozoic foliation in this rock, where present, is defined by flattening of quartz and feldspar grains and rare, thin (1–2 cm thick) aplite dikes that are concordant to metamorphic foliation.

The third type, garnet-bearing leucocratic granite gneiss (Ygt), is similar in appearance to Ygg but contains scattered garnets that compose less than 10 percent of the rock. Garnetiferous leucocratic gneiss is the dominant basement rock type immediately to the west and southwest of the map area (Southworth, 1991; Burton and others, 1992b). A fourth unit, biotitic Marshall Metagranite (Ymb), occurs in the southern part of the map area. It resembles biotitic

**Table 2.** Major oxide (weight percent) and trace-element (parts per million) geochemistry of four Middle Proterozoic rocks.

[n.d., not detected. All analyses, including X-ray spectroscopy, by U.S. Geological Survey; FeO, H<sub>2</sub>O, and CO<sub>2</sub> analysis by H. Smith, J.W. Marinenko, and J.R. Gillison; instrumental neutron activation analysis by G. Wandless and P. Baedeker]

| Major oxide                    | Map unit<br>Sample site <sup>1</sup><br>(sample number) |                       |                       |                      |
|--------------------------------|---|-----------------------|-----------------------|----------------------|
|                                | Ygg<br>1<br>(BR-11)                                     | Ybgg<br>2<br>(BR-554) | Yhp<br>3<br>(BR-602A) | Yrg<br>4<br>(BR-660) |
| SiO <sub>2</sub>               | 75.60   | 70.20                 | 50.50                 | 73.2                 |
| Al <sub>2</sub> O <sub>3</sub> | 13.00   | 13.80                 | 16.40                 | 11.3                 |
| Fe <sub>2</sub> O <sub>3</sub> | .65   | 1.72                  | 1.84                  | 1.1                  |
| FeO                            | .44   | 1.80                  | 5.60                  | 3.4                  |
| MgO                            | .22   | .74                   | 7.55                  | 1.73                 |
| CaO                            | .79   | 1.79                  | 11.30                 | 1.48                 |
| Na <sub>2</sub> O              | 3.41  | 2.68                  | 2.48                  | 2.72                 |
| K <sub>2</sub> O               | 5.11  | 5.04                  | .90                   | 1.32                 |
| TiO <sub>2</sub>               | .24   | .47                   | .65                   | .67                  |
| P <sub>2</sub> O <sub>5</sub>  | .05   | .18                   | .07                   | .06                  |
| MnO                            | .02   | .06                   | .13                   | .1                   |
| H <sub>2</sub> O <sup>+</sup>  | .29   | .62                   | 2.50                  | 1.7                  |
| H <sub>2</sub> O <sup>-</sup>  | .04   | .11                   | .01                   | n.d.                 |
| CO <sub>2</sub>                | n.d.  | n.d.                  | .01                   | n.d.                 |
| Total                          | 99.86   | 99.21                 | 99.94                 | 98.78                |
| Trace element                  | Abundance (parts per million)                           |                       |                       |                      |
| Scandium                       | 4.71  | 10.13                 | 36.5                  | 14.25                |
| Chromium                       | 8.2   | 19.6                  | 121                   | 76.7                 |
| Cobalt                         | 1.006   | 6.79                  | 46.4                  | 13.62                |
| Nickel                         | <12   | <31                   | 99                    | 45                   |
| Zinc                           | 16.3  | 68.9                  | 80                    | 92                   |
| Arsenic                        | <0.7  | <0.8                  | <0.05                 | <0.7                 |
| Selenium                       | <0.7  | <0.9                  | <2                    | n.d.                 |
| Rubidium                       | 83  | 174                   | 17.1                  | 40.2                 |
| Strontium                      | 104   | 136                   | 460                   | 226                  |
| Zirconium                      | 205   | 263                   | <70                   | 311                  |
| Molybdenum                     | <2  | <2                    | <5                    | <2                   |
| Antimony                       | <0.06   | <0.06                 | <0.1                  | .14                  |
| Cesium                         | .049  | .91                   | .3                    | <0.2                 |
| Barium                         | 659   | 778                   | 300                   | 357                  |
| Lanthanum                      | 41.1  | 38.1                  | 6.2                   | 46                   |
| Cerium                         | 76.2  | 68.2                  | 13.7                  | 90.6                 |
| Neodymium                      | 38  | 29.1                  | 8.7                   | 38.4                 |
| Samarium                       | 8.4   | 6.58                  | 2.39                  | 8.17                 |
| Europium                       | .863  | 1.26                  | 1.09                  | 1.49                 |
| Terbium                        | 1.109   | 1.18                  | .384                  | 1.16                 |
| Ytterbium                      | 2.53  | 3.89                  | 1.14                  | 4.31                 |
| Lutetium                       | .329  | .5                    | .178                  | .597                 |
| Hafnium                        | 5.91  | 7.43                  | .9                    | 7.73                 |
| Tantalum                       | .347  | .538                  | .089                  | .57                  |
| Gold                           | <4  | <4                    | <3                    | <2                   |
| Thorium                        | 2.58  | 2.89                  | .38                   | 12.09                |
| Uranium                        | .6  | .76                   | .2                    | 1.15                 |

<sup>1</sup> Sample site numbers refer to chemistry localities on plate 1.

granite gneiss (Yb<sub>gg</sub>) but is generally less well foliated. This unit has been traced south to the type area in the Marshall quadrangle (Burton and others, 1992b; P.T. Lyttle, U.S. Geological Survey, oral commun., 1991) as defined by Espenshade (1986). A sample of biotitic Marshall Metagranite (Ymb) from the Rectortown quadrangle yields a U-Pb isotopic age that differs significantly from one obtained from biotitic granite gneiss from the Waterford quadrangle, as discussed below (Aleinikoff and others, 1993).

White, coarse-grained, Middle Proterozoic quartz-plagioclase-microcline pegmatite of more than one intrusive generation is not shown but locally occurs as bodies 0.5 to 2 m thick. Folded and concordant bodies probably represent pre- and syntectonic phases, respectively, relative to Grenville high-grade metamorphism and deformation. Also well exposed along the Potomac River are tabular pegmatite dikes, which crosscut Middle Proterozoic foliation (fig. 2A). These undeformed dikes clearly represent a post-Grenville intrusive phase but are themselves cut by Late Proterozoic mafic dikes. They might correlate with the Late Proterozoic Robertson River intrusive suite to the south.

#### U-Pb AGES OF GRANITIC GNEISSES

As part of a regional geochronological study of the granitic gneiss units in the northern Blue Ridge anticlinorium, zircons were extracted from an exposure of the felsic granite gneiss (Y<sub>gg</sub>) along the Potomac River (sample 1, BR-11, in tables 1, 2; symbols 1 and U-1 on pl. 1); they yield a U-Pb age of  $1060 \pm 2$  Ma, which is thought to represent the time of intrusion and crystallization (Aleinikoff and others, 1993). An exposure of biotite granite gneiss (Yb<sub>gg</sub>) from the Waterford quadrangle (sample 2, BR-554, in tables 1, 2; symbols 2 and U-2 on pl. 1) yields a crystallization age of  $1055 \pm 5$  Ma (Aleinikoff and others, 1993). Garnetiferous leucocratic granite gneiss (Y<sub>gt</sub>) from the Harpers Ferry quadrangle yields an age of approximately 1,070 Ma (Aleinikoff and others, 1993). These three ages belong in the youngest group of dates (group 3) of Burton and others (1994). In contrast, a sample of biotitic Marshall Metagranite (Ymb) from the Rectortown quadrangle, southwest of the map area, yields an age of  $1110 \pm 4$  Ma, putting it in the older group 2 of Burton and others (1994).

#### LAYERED AND MAFIC GNEISSES

The Middle Proterozoic rocks include units of probable sedimentary and volcanic or mafic intrusive origin in association, and contrasting lithologically, with the granitic gneisses. These rocks are best exposed in Milltown and Catocin Creeks in the Waterford quadrangle.

The most abundant unit in this suite of rocks is a graphite-bearing, garnet-rich paragneiss (Y<sub>rg</sub>) (tables 1, 2; fig. 3). This rock is distinctively rusty weathering and

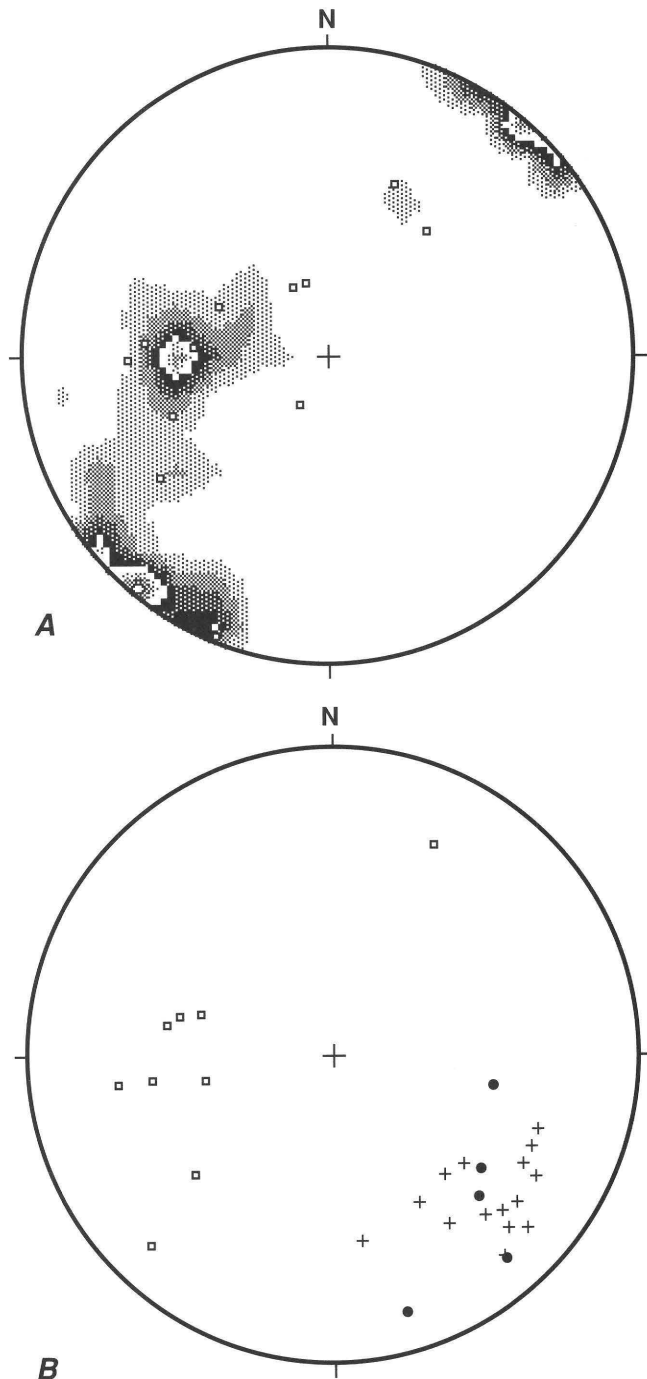


**Figure 2.** Lower hemisphere equal-area projections of structures of Middle Proterozoic age. *A*, Poles to foliation; contour interval is 2 percent per 1 percent area ( $n=90$ ); poles to tabular pegmatite veins ( $\blacksquare$ ,  $n=12$ ). *B*, Fold hinges ( $\bullet$ ,  $n=5$ ), mineral lineations ( $+$ ,  $n=15$ ), and poles to axial planes of isoclinal folds ( $\blacksquare$ ,  $n=9$ ).

contains a well-developed Middle Proterozoic layering defined by alternating quartz-plagioclase- and garnet-biotite (chlorite)-rich zones. It is locally migmatitic and has thin (1–3 cm) sills of aplite that are parallel to the layering. Although not always present, graphite occurs as evenly disseminated flakes less than 1 mm across. The original garnet

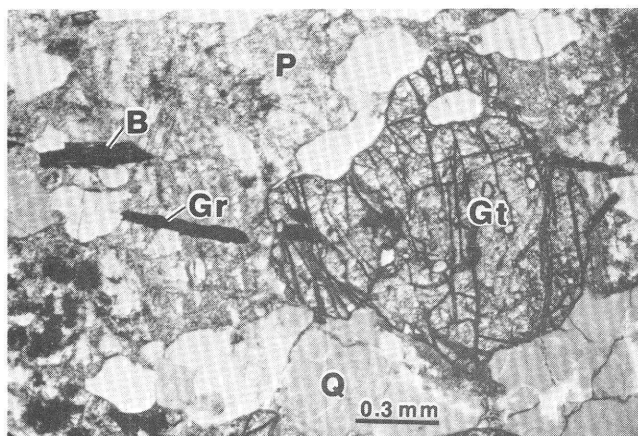


**Figure 3.** Photomicrograph showing thin section (plane polarized light) of garnet graphite paragneiss (Yrg), Waterford quadrangle. Minerals are garnet (Gt), graphite (Gr), chloritized biotite (B), sericitized plagioclase (P), and quartz (Q).

content was as much as 30 to 40 percent in some places; however, due to Paleozoic deformation, garnet is almost completely retrograded to green chlorite and is seen commonly only as smeared-out chlorite blebs. Biotite is retrograded commonly also to chlorite. High-grade aluminosilicate minerals such as sillimanite have not been found. Accessory minerals are locally common (as much as 15 percent) and include ilmenite, sphene (mantling ilmenite), apatite, rutile, and hematite. The mineralogy of the rusty paragneiss suggests that the protolith for this rock was an impure sandstone or graywacke containing some organic content (Burton and Southworth, 1993). The rusty paragneiss generally is poorly exposed but occurs in several quadrangles to the south and west (Burton and others, 1992b), indicating that it is a widespread unit in the Middle Proterozoic basement. This unit resembles the Border Gneiss of Hillhouse (1960) in the central Virginia Blue Ridge province, which is also garnet and graphite bearing, as described by Sinha and Bartholomew (1984) and Herz and Force (1984).

The second most important member of the suite is a hornblende-orthopyroxene-plagioclase gneiss or metanorite (Yhp; table 1; fig. 4). Metanorite was first recognized by Howard (1991; facies D), who mapped several small rounded bodies of it in the Waterford quadrangle. His map pattern for the metanorite is revised in this study. This mafic gneiss is a medium- to coarse-grained, massive rock that has an igneous-appearing texture. Orthopyroxene is the dominant mafic mineral, and hornblende is subordinate. Together with plagioclase they form a granoblastic texture typical of Middle Proterozoic (Grenvillian) rocks (fig. 4). In thin section the pyroxene is extensively uralitized and its original optical character almost completely obscured. The hornblende commonly is altered to colorless amphibole but where fresh is golden brown. Near contacts with granite

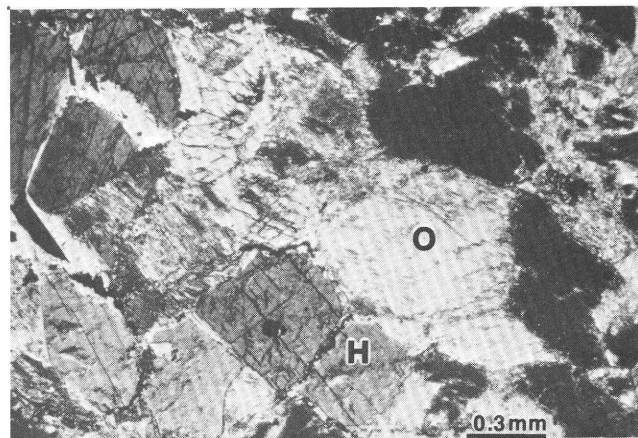


**Figure 4.** Photomicrograph showing thin section (crossed nicols) of hornblende metanorite (Yhp), Waterford quadrangle. Minerals are orthopyroxene (O), hornblende (H), plagioclase (large dark grains), and ilmenite (small black grains; opaque in thin sections).

gneiss, the hornblende-pyroxene gneiss locally changes to a fine-grained and well-layered charnockite (not mapped separately) with the addition of biotite, quartz, and microcline. Ilmenite, sphene, and apatite are local accessory minerals. The hornblende-pyroxene gneiss is assumed to have a mafic igneous origin. Its major oxide and trace-element geochemistry is shown in table 2. Burton and others (1992b) have mapped larger bodies of charnockite and metanorite to the west and southwest. Charnockite is much more abundant in the central Virginia Blue Ridge than in the northern part (Sinha and Bartholomew, 1984; Burton and others, 1992b), and the relative abundance of charnockite is one of the main differences between the two regions.

A minor unit within this suite of metasedimentary and metaigneous rocks is a gray, well-foliated to layered quartz-hornblende-biotite-plagioclase gneiss (Ybg). Where amphibole is locally the dominant mafic mineral, the rock is a metadiorite or amphibolite. Quartz content ranges from 0 to 10 percent; ilmenite and sphene (mantling ilmenite) are accessory minerals. The hornblende-biotite gneiss is commonly migmatitic, contains thin concordant granitic sills, and can grade imperceptibly into surrounding granitic gneiss. The protolith for this rock was probably a sediment having a volcanic component.

A fourth unit, quartz-plagioclase gneiss (Yqp), is a white- to gray-weathering felsic rock that ranges from massive to well foliated. It strongly resembles either Ybgg or Ygg in outcrop depending on biotite content but is characterized by little or no potassium feldspar, and its modal composition is that of a tonalite (table 1) or dacite. This unit is spatially associated with biotite granite gneiss (Ybgg), leucocratic granite gneiss (Ygg), and the layered and mafic gneisses. At one locality along Catoctin Creek, white, medium-grained, quartz-plagioclase gneiss is in contact with fine-grained amphibolite gneiss (Ybg) and contains

internal biotite- and amphibolite-rich layers; these layers suggest a mafic-felsic volcanic sequence. Quartz-plagioclase gneiss (Yqp) decreases in abundance southward from the Potomac River within the map area but is found northward to the nose of the basement core of the anticlinorium, according to reconnaissance by W.C. Burton (unpublished data, 1992). This rock resembles older (1300 Ma) trondhjemitic rocks that have been found in the Adirondacks (McClelland and Chiarenzelli, 1990), Green Mountains (Ratcliffe and others, 1991), and Reading Prong (Drake, 1984). However, U-Pb dating of zircon from a sample of this rock in Maryland puts it in the younger, group 3 intrusive suite (J.N. Aleinikoff, written commun., 1993).

The nongranitic rocks are interlayered with and enveloped by granite gneiss. Contacts between the two are concordant with respect to the regional Middle Proterozoic (Grenvillian) gneissic foliation and are probably pre- or syntectonic with respect to the Grenville orogeny; sharp crosscutting contacts are observed only for younger pegmatites. The present distribution and map pattern of the Middle Proterozoic units are thought to reflect partial melting of an older metasedimentary-metavolcanic terrane and intrusion by younger granites (Burton and Southworth, 1993). Mapping to the northwest, west, and southwest (Southworth, 1991; Burton and others, 1992b) indicates that the older, pregranitic rocks are volumetrically minor but widespread.

#### MIDDLE PROTEROZOIC FABRIC AND STRUCTURES

Although the Middle Proterozoic rocks of the Blue Ridge have undergone extensive overprinting by subsequent Paleozoic deformation and low-grade metamorphism, Middle Proterozoic metamorphic fabrics defined by high-grade mineral assemblages and structures are still clearly discernible in many places. At outcrop scale these features, and the rock types they are commonly found in, include a foliation defined by flattened mafic minerals such as biotite or less commonly hornblende (units Yb<sub>gg</sub>, Yb<sub>g</sub>) and flattened quartz and feldspar grains (Y<sub>gg</sub>); layering defined by concordant thin (1–10 cm) aplite or pegmatite sills (Y<sub>gg</sub>, Yb<sub>gg</sub>, Y<sub>qp</sub>, Y<sub>rg</sub>); biotite mineral lineation (Yb<sub>gg</sub>); and, rarely, open to isoclinal folds in metamorphic layering, the axial planes of which are parallel to the regional trend of foliation (Y<sub>rg</sub>, Yb<sub>g</sub>).

Petrographically, Middle Proterozoic textures are distinguished by the presence of a granoblastic elongate fabric, which has triple-junction grain boundaries, that is defined by mineral assemblages that are stable at granulite-facies metamorphic grade (figs. 3, 4), as well as the absence of a dominant penetrative fabric defined by low-grade minerals (muscovite, chlorite, epidote, actinolite). However, even in areas having a well-defined older fabric, static retrograde

alteration is ubiquitous due to Paleozoic and possibly Late Proterozoic low-grade (greenschist-facies) metamorphism. In thin section, plagioclase is commonly cloudy and has overgrowths of sericite or clinozoisite, garnet grains are reduced to fragmented cores that have chlorite rims, biotite may have chlorite intergrowths or opaque exsolution lamellae, hornblende has retrograded to colorless amphibole, and pyroxene is extensively uralitized.

Middle Proterozoic foliation in the map area has two main trends: a northwest trend with steep to moderate dips from the Potomac River to south of the Point of Rocks-Waterford quadrangle boundary and a more north-northeast trend with gentler dips in the rest of the Waterford quadrangle (fig. 2A). Rare, steeply plunging isoclinal folds are associated with and are axial planar to both foliation trends, and biotite granite gneiss (Yb<sub>gg</sub>) has a locally well-developed biotite lineation in both northeast and northwest trends. The biotite lineation, which is commonly parallel to rodded quartz and feldspar grains, suggests a stretching lineation. Significantly, the fold hinges, mineral lineations, and rodding associated with both foliation trends plunge southeast (fig. 2B). The poles to foliation (fig. 2A) appear to form a girdle around a pole approximately parallel to the mean of the fold axes and lineations (fig. 2B), which suggests that all these structures were affected or formed by a common tectonic event.

#### MIDDLE PROTEROZOIC METAMORPHISM

Mesoscopic and microscopic features in Middle Proterozoic rocks in the Blue Ridge basement, such as migmatitic layering and granoblastic mineral textures, clearly indicate high-grade metamorphic conditions during formation, and granulite-facies mineral assemblages are found in some lithologies in the map area. The presence of relict orthopyroxene and brown hornblende in textural equilibrium in hornblende-pyroxene gneiss (Y<sub>hp</sub>) (fig. 4) indicates hornblende granulite grade. A marginal facies of this gneiss that contains potassium feldspar is technically a charnockite—also diagnostic of granulite facies. Charnockitic rocks also are found elsewhere in the northern Blue Ridge basement (Howard, 1991; Southworth, 1991; Burton and others, 1992b). Well-developed Middle Proterozoic fabrics occur in both of the granitic gneiss samples from the map area dated by Aleinikoff and others (1993). Since these dates are presumably crystallization ages, it is reasonable to assume that at least some of the metamorphism and formation of associated metamorphic fabrics and structures is younger than about 1060 to 1055 Ma. Cooling ages from hornblende from Blue Ridge basement in northern Virginia are about 1000 to 900 Ma and represent minimum ages of metamorphism (Kunk and others, 1993). The bracketed age of metamorphism and deformation thus corresponds to the

late (Ottawan) phase of the Grenville orogeny of Moore and Thompson (1980).

### LATE PROTEROZOIC DIKES

The Middle Proterozoic gneisses in the core of the Blue Ridge anticlinorium are intruded by a dense swarm of northeast-trending, steeply southeast dipping Late Proterozoic dikes that are basaltic in composition (table 3), with the exception of two dikes that are rhyolitic in composition (Zr, pl. 1 and table 3). These dikes have long been recognized (for example, Furcron, 1939; Reed, 1955; Bartholomew, 1977), but a dike swarm of the density seen in this map area has not previously been mapped in such detail. The chemical composition of most of the dikes has led previous workers to consider them as feeders to the overlying metabasalts of the Catocin Formation (for example, Reed, 1955; Espenshade, 1986), a conclusion that is corroborated by this study.

#### DIKE LITHOLOGY

In the map area, two main types of mafic dikes were mapped on the basis of grain size and texture: fine- to medium-grained (grains up to 2 mm) metadiabase dikes (Zd) and medium- to coarse-grained (2–8 mm grain size) actinolitic metadiabase dikes (Zda). The mineral characterizing this difference in grain size is pale-green to colorless actinolite. In outcrop, the coarse-grained dikes (Zda) have a distinctive nubby surface texture due to the weathering out of stubby amphibole grains. In the map area, the actinolitic dikes (Zda) are confined largely to the eastern margin of the exposed basement and decrease in abundance southward. Fine- to medium-grained actinolitic metadiabase dikes in the basement have been mapped to the south and west by previous workers (Espenshade, 1986; Allen, 1963; Furcron, 1939), although some of the dikes are described as “amphibolites.” Those dikes have a maximum grain size of 2 mm (Lukert and Nuckols, 1976) and, therefore, probably correspond to the finer grained dikes (Zd) of this study. Truly coarse grained, gabbroic textured metabasic dikes, possibly correlative with Zda, have been reported only within cover-sequence metasedimentary and metavolcanic rocks to the south, including the “ultramafic rocks” of Allen (1963) and the “metagabbro” of Furcron (1939). Reconnaissance by Burton (unpub. data, 1992), however, has shown coarse-grained dikes to be present as well near the western margin of the basement core of the anticlinorium.

The original igneous texture and mineralogy of the mafic dikes Zd and Zda have been largely altered by a Paleozoic low-grade metamorphic event and deformation. In thin section the dominant minerals are those expected for a rock of basaltic composition metamorphosed under greenschist-facies conditions, namely chlorite, epidote, actinolite,

and altered plagioclase. The pale-green to colorless actinolite is the most abundant mineral in the coarse-grained dikes, making up 50 to 70 percent of the rock. Its stubby, equant character suggests that it is derived from primary, igneous pyroxene. Relict ophitic and subophitic texture is preserved locally in the form of thin elongate laths of altered plagioclase enclosed in the amphibole. The dominant fabric in both coarse- and fine-grained types is a closely spaced, anastomosing metamorphic foliation primarily composed of fine-grained chlorite, epidote, and muscovite. This fabric deforms and clearly postdates formation of the amphibole crystals. Greenish-brown biotite, stilpnomelane, and needle actinolite are also found. The significance of the metamorphic minerals and fabric is discussed further in the section on Paleozoic recrystallization and metamorphic grade.

A third dike lithology, Zr, is rhyolitic. Two such dikes were found; each was 1 to 3 m thick and could be traced along strike only a few meters. The best exposed rhyolite dike, along the Potomac River, is cream colored, has a dense, fine-grained, flinty texture, sharp planar margins, and an internal foliation parallel to the contacts, which originally may have been a primary flow foliation. The rhyolite dike intruded a metadiabase dike along one margin and thereby postdates it. In thin section it has a fine-grained, felted texture composed of microcrystalline quartz and potassium feldspar and scattered larger rounded grains of plagioclase. The foliation is marked by inclusion trains of fine-grained epidote, biotite, and hematite. Rhyolite dikes have also been reported elsewhere in the northern Virginia Blue Ridge basement (Southworth, 1991; Lukert and Nuckols, 1976).

A fourth type of dike, Zi, is porphyritic metadiabase containing abundant white to pink subhedral phenocrysts of plagioclase (now heavily saussuritized) 1 to 5 mm in length in a fine-grained groundmass of actinolite and chlorite. It appears more felsic in composition than the coarse- or fine-grained metadiabase dikes. A single body of this type was mapped north of Waterford, and its map pattern indicates that it cuts across the northeast-trending metadiabase dikes. Similar porphyritic dikes occur to the south and west (Klein and others, 1990; J.S. Schindler, U.S. Geological Survey, oral commun., 1991), but their petrogenetic significance is unknown.

#### DIKE DENSITY AND ORIENTATIONS

A fairly accurate rendering of the true distribution and density of the Late Proterozoic dikes can be seen best in cross section A–A' and the western part of cross section C–C' (pl. 1). In such areas of near-continuous exposure the dikes can be seen to vary in width from a few meters to a few tens of meters. Although a few narrow dikes are not shown, in these areas the map resolution is limited more by

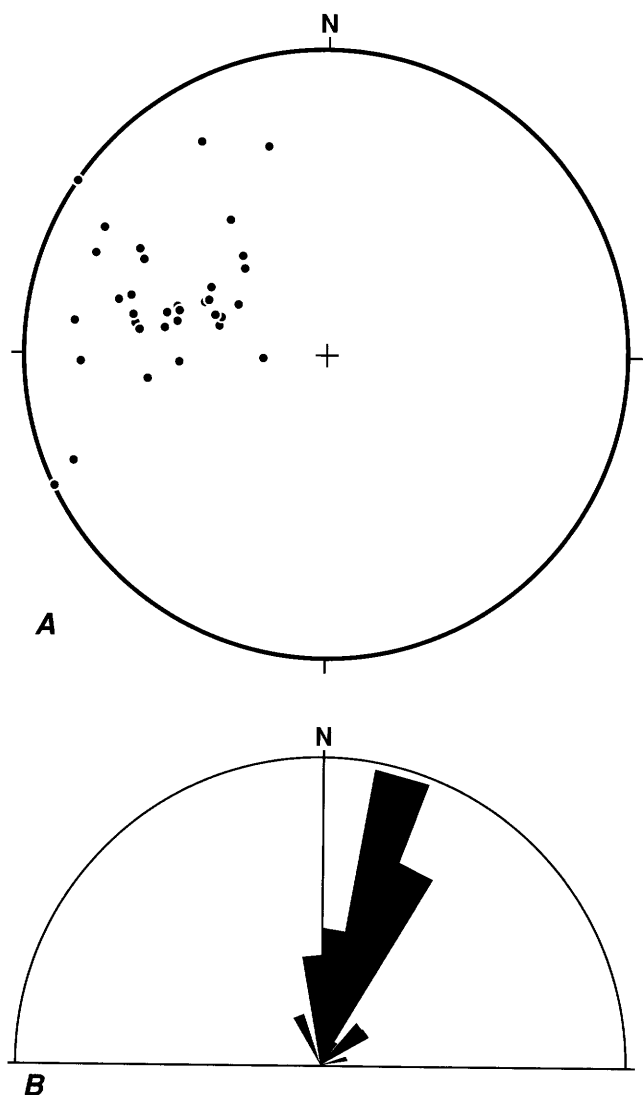


**Figure 5.** Orientation of Late Proterozoic dikes. A, Lower hemisphere equal-area projection of poles to exposed dike contacts (•, n=36). B, Rose diagram of contact azimuths.

gaps in exposure than by scale, and the dike pattern shown is generally correct. Elsewhere on the map there is much approximation and the dike-basement pattern is certainly far more complex than shown. In the best exposed section (A-A') along the Potomac bluffs, the metadiabase dikes make up about 60 percent of the exposed rock as measured across strike. Assuming that dike emplacement was by forceful intrusion and dilation rather than by stoping and assimilation, this locally implies a crustal extension of 150 percent.

The dikes were intruded into the crust in a northeast orientation, in accordance with a northwest extension direction during the opening of the Iapetus Ocean (Rankin, 1975). Figure 5 shows stereonet plots of the orientations of exposed dike margins in the field (fig. 5A) and azimuthal

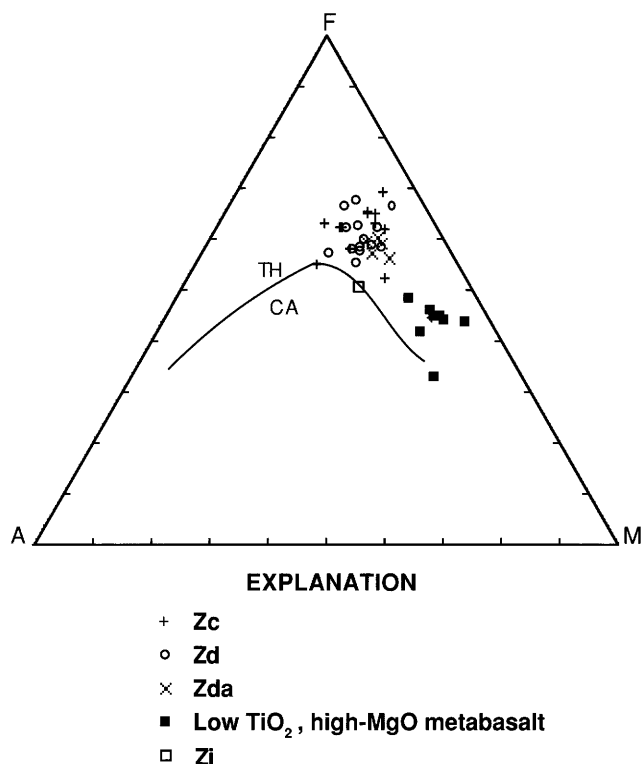


**Figure 6.** AFM diagram showing Late Proterozoic metadiabase and metabasalt. A, Na<sub>2</sub>O + K<sub>2</sub>O; F, total iron as FeO; M, MgO. Line separates tholeiitic (TH) from calc-alkaline (CA) field. Zc, metabasalt of the Catoctin Formation; Zd, fine-grained metadiabase dikes; Zda, coarse-grained metadiabase dikes; Zi, porphyritic metadiabase. Data from Espenshade (1986), Southworth (1991), P.T. Lyttle (U.S. Geological Survey, unpub. data), and table 3, this report.

trends of dikes (fig. 5B). Dike contacts, whether exposed or inferred on the map, are generally parallel to the dominant Paleozoic schistosity, suggesting either transposition or rotation of the dikes into parallelism with regional foliation during its development (Southworth, 1991), exploitation by the developing foliation of the previously existing dike-basement anisotropy, or both.

#### GEOCHEMISTRY

Major-oxide geochemical analyses of metadiabase dikes (Zd) and actinolite dikes (Zda) indicate that both types are of tholeiitic basalt composition (table 3, fig. 6). These rocks probably were relatively closed (isochemical) systems during metamorphism, as evidenced by the lack of features such as extensive veining and wall-rock alteration. The chemical composition of the porphyritic metadiabase (Zi) is on the boundary between the calc-alkaline and tholeiitic fields, according to the AFM diagram (fig. 6). Some chemical abundances in this rock, such as Al<sub>2</sub>O<sub>3</sub> (in weight percent) and Sr (in parts per million) (table 3), indicate that

**Table 3.** Major oxide (weight percent) and trace-element (parts per million) abundances and averages of Late Proterozoic metadiabase, metabasalt, and metarhyolite.

[n.d., not detected. All analyses, including X-ray spectroscopy, by U.S. Geological Survey; FeO, H<sub>2</sub>O, and CO<sub>2</sub> analysis by H. Smith, J.W. Marinenko, and J.R. Gillison; instrumental neutron activation analysis by G. Wandless and J. Mee]

| Major oxide                    | Map unit<br>Description<br>(sample number)<br>Sample site |              |              |                |               |                 |                |                 |                            |                |                |               | Averages<br>(no. of samples) |                 |                 |
|--------------------------------|---|--------------|--------------|----------------|---------------|-----------------|----------------|-----------------|----------------------------|----------------|----------------|---------------|------------------------------|-----------------|-----------------|
|                                | Zda   |              |              |                |               | Zd              |                |                 | Zi                         | Zc             |                | Zr            | Zda <sup>1</sup>             | Zd <sup>2</sup> | Zc <sup>3</sup> |
|                                | Actinolitic metadiabase                                   |              |              |                |               | Metadiabase     |                |                 | Porphyritic<br>metadiabase | Metabasalt     |                | Metarhyolite  | Actinolitic<br>metadiabase   | Metadiabase     | Metabasalt      |
|                                | (BR-2)<br>5   | (BR-67)<br>6 | (BR-82)<br>7 | (BR-452A)<br>8 | (BR-738)<br>9 | (BR-452B)<br>10 | (BR-226)<br>11 | (BR-610A)<br>12 | (BR-681)<br>13             | (BR-117)<br>14 | (BR-807)<br>15 | (BR-38)<br>16 | (5)                          | (14)            | (13)            |
| SiO <sub>2</sub>               | 45.40   | 44.60        | 46.40        | 46.80          | 46.90         | 46.70           | 46.10          | 48.60           | 48.70                      | 47.20          | 45.90          | 74.20         | 46.02                        | 48.24           | 48.02           |
| TiO <sub>2</sub>               | 1.98  | 2.31         | 2.18         | 2.42           | 1.97          | 2.53            | 2.18           | 2.62            | 1.34                       | 2.28           | 2.66           | .19           | 2.17                         | 2.48            | 2.57            |
| Al <sub>2</sub> O <sub>3</sub> | 14.50   | 14.00        | 14.00        | 13.70          | 15.10         | 13.50           | 13.90          | 13.50           | 17.40                      | 14.00          | 13.20          | 12.60         | 14.26                        | 13.82           | 14.08           |
| Fe <sub>2</sub> O <sub>3</sub> | 3.80  | 3.74         | 3.76         | 3.61           | 3.42          | 3.83            | 2.53           | 2.51            | 2.97                       | 5.08           | 5.38           | 1.32          | 3.67                         | 3.60            | 6.49            |
| FeO                            | 9.10  | 10.50        | 9.40         | 9.90           | 8.90          | 9.70            | 10.60          | 11.70           | 6.20                       | 7.40           | 9.20           | .76           | 9.56                         | 9.45            | 7.36            |
| MnO                            | .20   | .24          | .22          | .22            | .20           | .22             | .22            | .22             | .15                        | .19            | .24            | .02           | .22                          | .20             | .22             |
| MgO                            | 7.67  | 6.97         | 6.92         | 6.47           | 6.55          | 6.11            | 6.94           | 5.56            | 5.61                       | 6.12           | 6.46           | .25           | 6.92                         | 5.63            | 6.41            |
| CaO                            | 11.10   | 10.30        | 11.20        | 10.40          | 11.00         | 10.70           | 11.20          | 10.50           | 11.30                      | 10.80          | 11.20          | 1.32          | 10.80                        | 10.34           | 7.46            |
| Na <sub>2</sub> O              | 1.81  | 2.54         | 2.47         | 2.76           | 2.69          | 2.76            | 2.54           | 2.39            | 3.01                       | 1.88           | 2.13           | 3.71          | 2.45                         | 2.46            | 2.74            |
| K <sub>2</sub> O               | .78   | .20          | .12          | .36            | .26           | .45             | .12            | .71             | .47                        | .05            | .28            | 4.33          | .34                          | .64             | .53             |
| H <sub>2</sub> O <sup>+</sup>  | 2.80  | 2.90         | 2.50         | 2.10           | 3.20          | 2.10            | 2.20           | 1.40            | 2.80                       | 3.00           | 3.30           | .27           | 2.70                         | 2.23            | 3.01            |
| H <sub>2</sub> O <sup>-</sup>  | .20   | .03          | .06          | .01            | .02           | .06             | .09            | .04             | .03                        | .11            | .04            | .02           | .06                          | .18             | .20             |
| P <sub>2</sub> O <sub>5</sub>  | .18   | .32          | .23          | .36            | .24           | .34             | .24            | .30             | .15                        | .21            | .39            | .05           | .27                          | .31             | .29             |
| CO <sub>2</sub>                | .01   | .01          | n.d.         | n.d.           | .01           | n.d.            | n.d.           | .01             | .01                        | 1.00           | .01            | n.d.          | .01                          | n.d.            | .08             |
| Total                          | 99.53   | 98.66        | 99.46        | 99.11          | 100.46        | 99.00           | 98.86          | 100.06          | 100.14                     | 99.32          | 100.39         | 99.04         | 99.44                        | 99.58           | 99.45           |
| Trace element                  | Abundance (parts per million)                             |              |              |                |               |                 |                |                 |                            |                |                |               |                              |                 |                 |
| Scandium                       | 39.1  | 38.2         | 40.8         | 43.6           | 37.6          | 41.9            | 38.9           | 35.9            | 29.3                       | 34.9           | 42.5           | 1.8           |                              |                 |                 |
| Chromium                       | 163   | 72.1         | 182          | 207            | 159           | 153             | 139            | 37.7            | 154                        | 134            | 131            | 10.2          |                              |                 |                 |
| Cobalt                         | 51.1  | 51           | 42.9         | 44.5           | 39.3          | 42.2            | 43.9           | 50              | 31.4                       | 47.4           | 45             | 1.3           |                              |                 |                 |
| Nickel                         | 104   | 92           | 89           | 78             | 71            | 62              | 89             | 56              | 35                         | 104            | 69             | 9.9           |                              |                 |                 |
| Zinc                           | 77  | 93           | 78.8         | 85             | 105           | 90              | 84             | 125             | 78.7                       | 71             | 126            | 62.4          |                              |                 |                 |
| Arsenic                        | <1  | <0.9         | 4.5          | <1             | <0.7          | <2              | <1             | 1.04            | <0.7                       | <1             | <0.6           | <1            |                              |                 |                 |
| Selenium                       | <2  | <3           | <1           | <2             | <5            | <2              | <2             | <4              | <0.7                       | <2             | <2             | <1            |                              |                 |                 |
| Rubidium                       | 20  | <7           | <7           | 16.7           | 7.5           | 17              | 14.4           | 26              | 12                         | <7             | 11.2           | 81.1          |                              |                 |                 |
| Strontium                      | 446   | 330          | 320          | 330            | 370           | 350             | 300            | 330             | 430                        | 280            | 291            | 180           |                              |                 |                 |
| Zirconium                      | 190   | 160          | <200         | 151            | <500          | <260            | 125            | <500            | 140                        | 200            | 200            | 447           |                              |                 |                 |
| Molybdenum                     | <4  | <7           | <6           | <4             | <7            | <5              | <5             | 5.4             | <5                         | <4             | <6             | 2.9           |                              |                 |                 |
| Antimony                       | <0.1  | <0.1         | <0.1         | <0.1           | .12           | <0.1            | <0.1           | <0.08           | <0.09                      | .16            | <0.1           | .51           |                              |                 |                 |



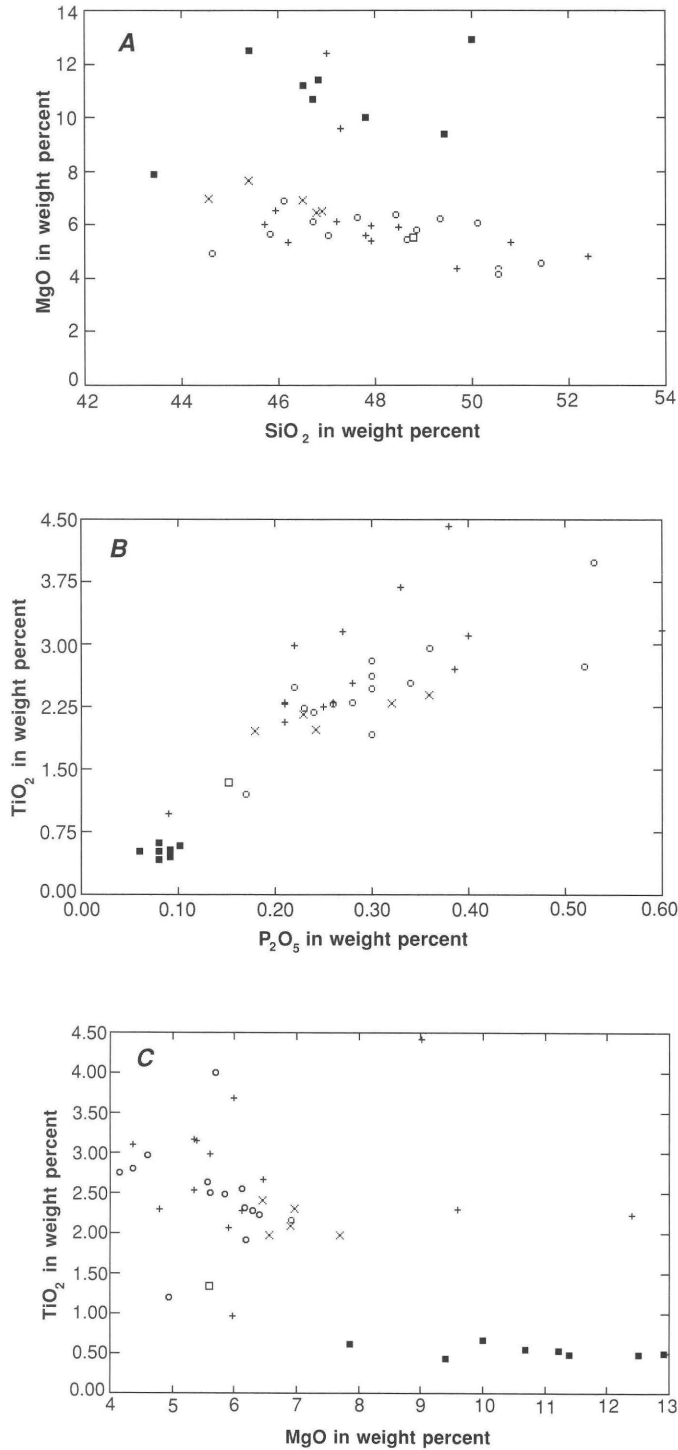


**Figure 7.** Variation diagrams of Late Proterozoic metadiabase and metabasalt. A, MgO versus SiO<sub>2</sub>. B, TiO<sub>2</sub> versus P<sub>2</sub>O<sub>5</sub>. C, TiO<sub>2</sub> versus MgO. Zc, metabasalt of the Catoctin Formation; Zd, fine-grained metadiabase dikes; Zda, coarse-grained metadiabase dikes; Zi, porphyritic metadiabase. Data from Espenshade (1986), Southworth (1991), P.T. Lyttle (U.S. Geological Survey, unpub. data), and table 3, this report.

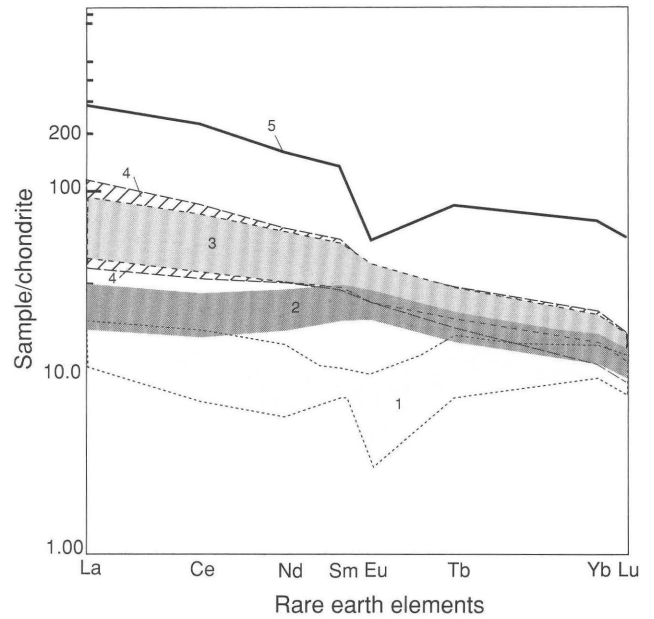


**Figure 8.** Chondrite-normalized REE diagram of Late Proterozoic metadiabase and metabasalt. 1, low-TiO<sub>2</sub>, high-MgO metabasalt; 2, coarse-grained actinolitic metadiabase dikes (Zda); 3, fine-grained metadiabase dikes (Zd); 4, metabasalt of the Catoctin Formation (Zc); and 5, metarhyolite dike (Zr). La, lanthanum; Ce, cerium; Nd, neodymium; Sm, samarium; Eu, europium; Tb, terbium; Yb, ytterbium; Lu, lutetium. Data from Espenshade (1986), Southworth (1991), P.T. Lyttle (U.S. Geological Survey, unpub. data), and table 3, this report.

these is indeed the subaerial product of the dated rhyolite dike then the maximum age for Catoctin rocks stratigraphically above these tuffs is about 572 Ma.

## LATE PROTEROZOIC METASEDIMENTARY AND METAVOLCANIC ROCKS

### SWIFT RUN FORMATION

The Swift Run Formation is a thin sequence of clastic and tuffaceous metasediments that nonconformably overlies the Middle Proterozoic gneisses of the basement along most of the eastern margin of the basement core of the Blue Ridge anticlinorium in the map area. The Swift Run, defined in this area as the cover sequence below the lowermost metabasalt, is thickest at the southern end of the map area (about 305 m; cross section *D-D'*, pl. 1) and thins gradually to the north where it pinches out in places beneath the Catoctin Formation. Along the Potomac bluffs, the Swift Run Formation appears to have been tectonically removed (see "Possible Rift-Related Faults" below). Just to the north

in Maryland, it is restricted to scattered lenses (Farth and Brezinski, 1994; Jonas and Stose, 1938) and reaches its maximum thickness on the western limb of the Blue Ridge anticlinorium in Virginia (Southworth, 1991).

The basal cover-sequence metasedimentary unit farther south along the eastern limb of the Blue Ridge anticlinorium is known as the Fauquier Formation, which is characterized mainly by a sequence of crossbedded arkoses, interbedded siltstone and sandstone, and rhythmically bedded siltstones (Espenshade, 1986; Klein and others, 1990). The boundary between the Fauquier and Swift Run Formations is placed at two east-trending, synsedimentary(?) faults in the Lincoln quadrangle; one marks the southern termination of the Swift Run Formation, and the other marks the northern extent of the Fauquier Formation. The Catoctin Formation rests on basement in between (Burton and others, 1992b).

The Swift Run Formation in the map area has two principle members: a basal member composed of quartz-pebble-bearing metasandstone, metaconglomerate, and pebbly quartz-muscovite phyllite (Zsq) and an overlying fine-grained quartz-muscovite phyllite (Zst). The pebbly member (Zsq) is discontinuous and is only a few meters thick at its maximum. It is characterized by the presence of scattered blue-quartz pebbles several millimeters in diameter in a finer grained matrix. An exposure in the southern Waterford quadrangle just north of Paeonian Springs contains a 1-m thick bed, which contains white quartz pebbles as much as 3 cm in diameter and which is the only coarse-grained Swift Run lithology exposed in the map area.

Overlying this basal member is the fine-grained quartz-muscovite phyllite, which lacks quartz pebbles. This unit is thicker and more widespread and is distinctive in outcrop and float as a conspicuous, creamy-white lustrous schist. Its fine grain size and felsic composition suggest a felsic tuff and (or) tuffaceous sediment as protolith.

About 30 to 40 m above the basal unconformity is a discontinuous layer as much as several meters thick of buff- to brown-weathering, white calcite marble. This marble occurs within the tuffaceous member of the Swift Run Formation in the southern part of the map area (Zsm), and a similar marble (Zcm) occurs within metabasalts of the Catoctin Formation to the north. If these marbles represent a single lithostratigraphic horizon then the tuffaceous rocks to the south and lowermost metabasalts to the north are time-stratigraphic equivalents. The section of tuffaceous Swift Run Formation (Zst) would thus grade laterally into the sequence of intercalated metabasalt (Zc) and felsic metatuff or tuffaceous metasediment (Zct) in the lower part of the Catoctin Formation near the Potomac River. To the south of the map area, marble occurs somewhat higher in the section, just above or below the contact between the Swift Run or Fauquier Formations and the Catoctin Formation (Espenshade, 1986; Klein and others, 1990; Burton and others, 1992b). The apparent change in stratigraphic position of the

marble (assuming a single marble horizon) and the change from Swift Run to Fauquier lithologies suggest significant changes in sedimentation from north to south before deposition of the Catoctin.

The depositional environment for the Swift Run Formation in this region was clearly one of low energy and small topographic gradients, as evidenced by the absence of thick clastic sediments, by the prevalence of fine-grained sediments and (or) volcanic rocks, and by the presence of a marble horizon. The tuffaceous upper member of the Swift Run Formation possibly represents early, distal ash-fall deposits, which mostly preceded the voluminous outpouring of basalt during formation of the Catoctin.

### CATOCTIN FORMATION

The Catoctin Formation in the Waterford and Point of Rocks quadrangles is characterized primarily by metabasalt (greenstone), as it is regionally (Espenshade, 1986; Klein and others, 1990), but a number of other lithologies occur as well, particularly in the lower part. The lower part of the Catoctin is best exposed in lower Catoctin Creek, just before it enters the Potomac River. Here the formation contains dark-green, fine-grained metabasalt (Zc) and coarse-grained, actinolitic metabasalt or metadiabase (Zca), white lustrous fine-grained quartz-muscovite phyllite, interpreted as metamorphosed tuff or tuffaceous metasediment (Zct), buff-weathering, fine- to medium-grained, greenish- or bluish-white calcite marble (Zcm), and fine- to medium-grained yellow- to white-weathering, crossbedded plagioclase-quartz metasandstone (Zcs). Farther south only the marble and discontinuous horizons of metasandstone were mapped in the lower Catoctin, whereas the tuffaceous horizons may have their lateral equivalent in the Swift Run Formation (Zst), as stated above. Scattered throughout the Catoctin are submeter-wide zones of alternating light- and dark-colored, centimeter-scale quartz-rich and mafic layers, testifying to local episodes of sedimentation during eruption of the Catoctin basalts.

An enigmatic rock type in the lower part of the Catoctin is a coarse-grained, actinolitic metamafic rock, which strongly resembles the coarse-grained dikes in the basement (Zda). Pale-green to colorless actinolite is the dominant mineral in thin section, forms porphyroblasts as much as 1 to 2 cm in diameter, and is accompanied by lesser chlorite and epidote. The coarse-grained Catoctin is interpreted here to be of two origins. Near the base of the Catoctin, where coarse-grained actinolitic rock is mapped as crosscutting other units, it is indeed considered intrusive (Zda). Higher in the section, coarse-grained zones seem to follow the regional trend of the layering as defined by the metasandstone and are interpreted as coarse-grained flow interiors (Zca). A problem with the latter interpretation is that such coarse-grained rocks are absent from the upper part of the

Catoctin where metabasalt is more predominant and such features should be more abundant.

In the southern part of the map area, coarser grained mafic rocks mostly are absent, and the continuum of metabasalt in the lower part of the Catoctin is broken only by discontinuous thin lenses of metasandstone. The upper part of the Catoctin, however, contains another metasedimentary unit, Zcp, which is quartzose phyllite. It is composed of fine-grained quartz, biotite, muscovite, epidote, and magnetite and, locally, graphite. Zcp has a slabby habit in outcrop, and its relative lack of green minerals such as chlorite distinguishes it from the surrounding metabasalt. The phyllite unit is best exposed in the upper Limestone Branch and pinches out to the north and south.

The Catoctin in the southern part of the map area is more than twice as thick (nearly 7,000 ft; section *D-D'*, pl. 1) as that near the Potomac River (2,700 ft; section *B-B'*, pl. 1). This may be due in part to the presence of metasediments such as phyllite (Zcp) but more likely reflects thickening of metabasalt to the south, a trend which continues south into the Lincoln quadrangle (Burton and others, 1992b). A later tectonic influence on thickness in the form of large-scale isoclinal folds is unlikely, however, due to the compositional asymmetry of the lower and upper part of the Catoctin. However, unrecognized north-trending Mesozoic normal faults, which would increase the apparent thickness, cannot be ruled out. Along with the change in thickness, differences between the Catoctin as mapped in the northern part and the southern part include (1) lack of felsic tuffaceous units above the lowest metabasalt in the south, as opposed to the north, (2) apparent lack of any coarse-grained mafic units in the lower part of the Catoctin in the south, and (3) a mappable phyllitic layer in the upper part of the Catoctin in the south. These along-strike variations testify to lateral changes in conditions during deposition of the Catoctin protolith.

Epidosite, a fine-grained, massive, yellowish-green rock consisting of epidote and quartz, is widespread but restricted to the fine-grained metabasalt of the Catoctin Formation (Zc). It typically occurs as discontinuous layers or boudins as much as a few meters in length that are enclosed in greenstone, and it is considered to be an alteration product of the metabasalt (Reed and Morgan, 1971). Due to a resistance to erosion, it is abundant as float boulders. The epidosite commonly has relict amygdules filled with quartz or less commonly calcite, albite, or biotite. The amygdules appear to be relict primary features, suggesting that the epidosite preferentially formed from scoriaceous lava, perhaps at the tops and bottoms of flows, where fluids could more easily circulate. The pinched and boudinaged nature of the epidosite indicates that the alteration occurred prior to Paleozoic deformation, but whether the alteration itself is Paleozoic or older is unknown.

As stated above, the four thin felsic metatuff layers (Zct) near the base of the Catoctin Formation represent the

nearest known extrusive equivalents to a rhyolite dike in the basement (Zr) that has been dated at  $572 \pm 5$  Ma. This suggests that the upper part of the Catoctin Formation is younger than that age.

#### POSSIBLE RIFT-RELATED FAULTS

The dike complex intruding Middle Proterozoic basement rocks and the Catoctin Formation metabasalts overlying the basement are the most visible products of the Late Proterozoic crustal rifting event that occurred along the eastern margin of the craton during the opening of the Iapetus Ocean (Rankin, 1975). Normal faults associated with the widespread crustal extension that is presumed to have accompanied this event, however, have been difficult to pinpoint in this region, probably due to subsequent reactivation and obliteration during the compressional event(s) of the Paleozoic. Espenshade (1986) and Klein and others (1990, 1991) have mapped cross-strike and along-strike faults in the Marshall quadrangle to the south, which they consider to be rift related.

In this map area (pl. 1), two east-dipping mylonite zones were mapped that in thin section show kinematic indicators of a normal, down-to-the-east sense of movement (sections *A-A'*, *C-C'*, pl. 1). In terms of mineralogy and field aspect these mylonites are indistinguishable from reverse-sense (up to the west) mylonites also mapped (section *C-C'*). The chlorite- to biotite-grade mineral assemblages seen in thin sections of these apparent normal fault-zone mylonites also resemble those associated with Paleozoic compressional deformation. Therefore, despite their normal movement sense, these faults are considered to be coeval with the Paleozoic reverse faults.

Perhaps more convincing evidence for normal faulting associated with rifting is found just above the basal unconformity between metatuff of the Catoctin Formation (Zct) and an underlying basement dike (Zd) along the Potomac River. Although no outcrop occurs, a narrow fault zone is evidenced by float blocks of dark-green, mylonitic greenstone of the Catoctin (Zc) containing angular clasts, one to several centimeters in diameter, of white fine-grained marble. The marble clasts are probably derived from marble of the Catoctin (Zcm). The missing section implied by the proximity of the marble to basement (as much as 100 m) suggests that this fault zone reflects either west-over-east reverse faulting or east-side-down normal faulting. The latter interpretation is adopted on the map. This mylonite zone cannot be traced any distance southward due to exposure, but Jonas and Stose (1938) found a similar zone along strike north of the Potomac River. Significantly, the mylonite contains tight kink folds that resemble folds in the Paleozoic cover-sequence rocks, suggesting that Paleozoic compression occurred subsequent to faulting.

## CHILHOWEE GROUP METASEDIMENTARY ROCKS

### LOUDOUN FORMATION

There has been discussion over the years about the possible presence or absence of a mappable metasedimentary unit between the Catoctin Formation metabasalts and the clean Weverton Quartzite. Keith (1894) and Jonas and Stose (1938) recognized such a unit but also mistakenly mapped some metasedimentary rocks in the Catoctin and the basal cover-sequence metasediments of the Fauquier and Swift Run Formations as infolds of the Loudoun Formation. Whittaker (1955) correctly mapped the Loudoun Formation metasediments between the Catoctin and Weverton and found it pinching out south of the Potomac River. Nickelsen (1956) likewise mapped the Loudoun between the Catoctin and Weverton on the western limb of the Blue Ridge anticlinorium. Nunan (1979), in contrast, concluded that the Loudoun Formation was not a mappable unit and included the metasediments above the metabasalts within the basal Weverton. Reed (1955) on the other hand thought that phyllites in this stratigraphic position represented metamorphosed saprolite developed on the Catoctin. The present study agrees with Whittaker as to both the validity of the Loudoun Formation and its pinching out to the south. On this map (pl. 1), the formation pinches out just south of the Waterford–Point of Rocks quadrangle boundary, about 3 km north of where Whittaker terminated it. The Loudoun Formation is here considered to be the basal unit, at least locally, of the Chilhowee Group and has a maximum thickness in the map area of about 30 m.

The Loudoun Formation (€l) is best exposed on the east-facing slope of Catoctin Mountain west of U.S. Route 15 and just south of the Point of Rocks bridge. The contact of the Loudoun with the underlying Catoctin Formation is a gradational zone marked by interlayered greenstone and distinctive, bluish-black phyllite layers from 10 cm to 1 to 2 m thick (the “purple phyllite” of Whittaker, 1955). These fine-grained black phyllites also are distinctive compositionally and consist mostly of muscovite and graphite and lesser amounts of chlorite and quartz. The Loudoun Formation proper, overlying the uppermost metabasalt, is an extremely variegated unit containing phyllite, phyllitic metaconglomerate and pebbly metasandstone, and minor vitreous quartzite (fig. 9). Loudoun Formation phyllite in contact with Catoctin Formation metabasalt is exposed in the roadcut on U.S. Route 15, where it is a chlorite-quartz-muscovite phyllite, containing minor amounts of magnetite and graphite, and contains quartzite layers as much as 1 m thick. More quartz-rich lithologies, including phyllitic metasandstone and metaconglomerate, and a 3- to 4-m thick vitreous quartzite layer are found upslope and upsection (west). These units apparently pinch out southward along with the formation as a whole; the southernmost exposures

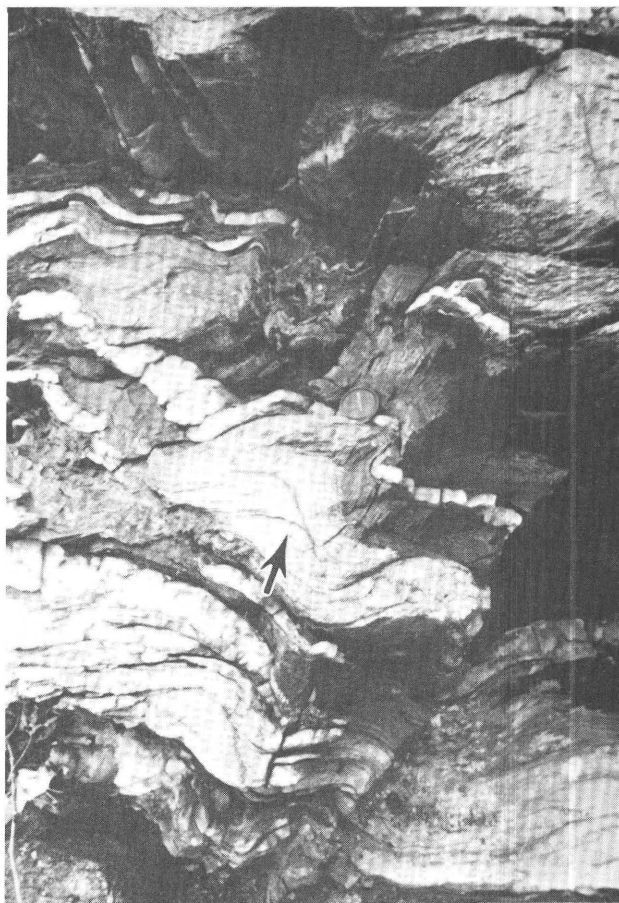


**Figure 9.** Recumbent, isoclinal  $F_1$  folds (arrow) and more open, upright  $F_2$  folds with associated steeply dipping crenulation cleavage in interlayered phyllite and quartzite of the Loudoun Formation, at the northern end of Catoctin Mountain (Virginia portion), just south of U.S. Route 15 bridge over the Potomac River, Point of Rocks quadrangle. View looking south approximately parallel to azimuths of fold hinges; lens cap diameter is 5 cm.

of Loudoun Formation consist solely of graphite-quartz-muscovite phyllite. An outcrop on the northern face of Catoctin Mountain, interpreted as the exposed contact between the Loudoun Formation and Weverton Quartzite, contains thickly bedded, white vitreous quartzite in contact with and overlying black phyllite. This study could not corroborate Whittaker's (1955) subdivision of the Loudoun Formation into an upper conglomeratic member and a lower phyllitic member.

### WEVERTON QUARTZITE

The Weverton Quartzite (€w) in the map area is a grayish-white- to cream-weathering, massive to thickly bedded vitreous orthoquartzite about 30 to 46 m thick. The thinness and uniformity of the Weverton Quartzite in the map area contrasts with the formation as mapped on the

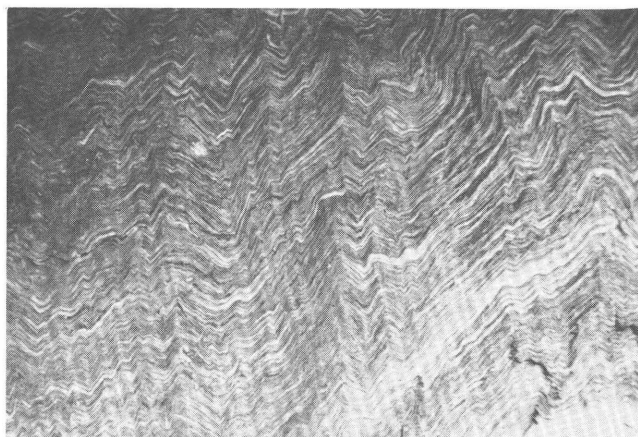


**Figure 10.** Outcrop on the western flank of Catoctin Mountain, just east of Furnace Mountain, showing upright, post- $F_2$  kink folds in  $S_1$ -laminated quartzose phyllite of the Harpers Formation. View looking north approximately parallel to strike of axial planes of kink folds; area is about 1 m across.

western limb of the anticlinorium (Nickelsen, 1956) and to the north in Maryland (Whittaker, 1955), where three members are recognized. Lithologic variation in the Weverton Quartzite here consists of minor thin (less than 10 cm) interbeds of dark phyllite and sugary-white-weathering pebbly layers 1 to 2 m thick. Bedding is typically marked by very fine dark laminae, which commonly outline crossbeds and scour and fill structures; these yield the topping directions shown on the map. The contact of the Weverton with the underlying Loudoun or Catoctin Formations is apparently sharp; the contact with the overlying Harpers Formation is gradational. No evidence for an angular unconformity beneath the Weverton could be found; however, the apparent pinching out of the Loudoun Formation under the Weverton Quartzite may be a result of erosion before or in the earliest stages of deposition of the Weverton.

#### HARPERS FORMATION

The Harpers Formation ( $\epsilon h$ ) is a fine-grained, well-foliated chlorite-biotite-muscovite-quartz phyllite (figs. 10, 11). Its thickness ranges from about 500 ft in the Point of Rocks quadrangle (section  $B-B'$ , pl. 1) to more than 2,000 ft in the Waterford quadrangle (section  $C-C'$ , pl. 1). Harpers Formation phyllite is distinguished from phyllite of the Loudoun Formation by the abundance of quartz, the presence of biotite, and the absence of graphite. Magnetite is locally abundant. The phyllite commonly contains conspicuous, millimeter-scale, alternating light and dark laminae, which are quartz rich and mica rich, respectively. A meter-thick quartzose layer sampled in the Harpers Formation is composed of quartz, potassium feldspar, and plagioclase

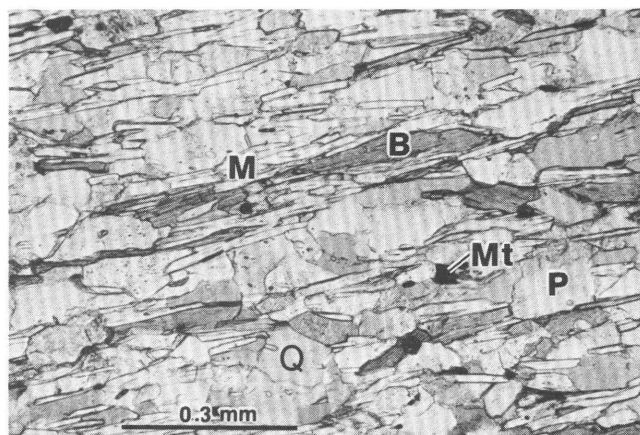


**Figure 11.** Photomicrograph showing thin section (plane polarized light) of well-developed  $S_1$  in quartzose phyllite of the Harpers Formation, Point of Rocks quadrangle. Minerals are biotite (B), muscovite (M), quartz (Q), plagioclase (P), and magnetite (Mt).

and is similar in composition to the overlying Antietam Quartzite. No mappable subdivisions could be distinguished within the Harpers Formation; lithologic variation consists of gradual, slight variations in quartz and mica content. More quartz-rich phyllite occurs just above the Weverton Quartzite and immediately below the Antietam Quartzite, with which the Harpers has gradational contacts.

#### ANTIETAM QUARTZITE

The Antietam Quartzite ( $\epsilon a$ ) is a poorly exposed, gray- to buff-weathering, massive, fine-grained meta-arkose about 100 ft thick. It is composed of roughly 45 percent quartz, 30 percent potassium feldspar, and 25 percent plagioclase. Physiographically the Antietam forms a topographic high in contrast to the phyllite of the Harpers Formation ( $\epsilon h$ ) and carbonate of the Tomstown Dolomite ( $\epsilon t$ ) between which it occurs. At Furnace Mountain, the Antietam Quartzite is the host rock for deposits of limonite that were mined for iron ore in the 19th century (Holden, 1907) and have an irregular distribution, as indicated by the old mine pits of Furnace Mountain (limonite-quarry and limonite-prospect symbols on pl. 1).

#### POST-CHILHOWEE GROUP METASEDIMENTARY ROCKS

##### CARBONACEOUS PHYLLITE

Overlying the Antietam Quartzite in places, but poorly exposed, is a very fine grained, sooty gray to black carbonaceous phyllite ( $\epsilon cp$ ). The phyllite locally contains light and dark laminae suggesting bedding. In thin section

quartz-rich zones alternate with feathery micaceous zones consisting of fine-grained sericite and finely disseminated carbonaceous material. Fine-grained sulfides are also present. The rock is notable for the acidic ground water it generates (James Athey, oral commun., 1990). The maximum thickness for the carbonaceous phyllite is probably less than 61 m.

The carbonaceous phyllite occurs in the same stratigraphic position as the lower part of the Tomstown Dolomite and apparently interfingers with it. The map pattern indicates that this lateral change from dolomite to phyllite occurs on a scale of a few tens of meters, perhaps suggesting extremely localized euxinic basins in which a black mud was deposited that later formed the phyllite. The unit may be equivalent to a thin black phyllite, 5 to 10 m thick, recognized in the uppermost part of the Araby Formation (equivalent to the Antietam) in Maryland, just below the lowermost carbonate (Reinhardt, 1974).

#### TOMSTOWN DOLOMITE AND FREDERICK LIMESTONE

Overlying the Antietam Quartzite and perhaps laterally equivalent to the carbonaceous phyllite (€cp) is the Tomstown Dolomite (€t), a gray- to buff-weathering fine-grained dolomite that has a white to bluish-gray fresh surface. Bedding, where visible, ranges in style and thickness from coarse beds 10 to 20 cm thick to fine millimeter-scale light and dark laminae. Sandy layers are locally present. The dolomite is well exposed in fields near the Potomac River, where it is in contact with the underlying Antietam Quartzite and the overlying Frederick Limestone. The contact with the quartzite is sharp and well defined, whereas the contact with the limestone is gradational (J. Reinhardt, oral commun., 1991). Another exposure of Tomstown Dolomite is in a creek southwest of Furnace Mountain, where it is separated from the Harpers Formation by a normal fault (Furnace Mountain fault). Southward, the dolomite grades laterally into carbonaceous phyllite (€cp), which, along with the dolomite and the underlying Antietam Quartzite, is truncated by the early Mesozoic Bull Run fault. The maximum thickness of the Tomstown is the same as that for the carbonaceous phyllite.

The Frederick Limestone (€f) is exposed only in fields just south of the Potomac River in the map area. Strongly resembling the Tomstown Dolomite in appearance, it is gray weathering, bluish gray, well bedded to finely laminated, and in these exposures highly folded. Due to this deformation, a stratigraphic thickness cannot be estimated.

#### PALEOZOIC STRUCTURE AND METAMORPHISM

The Proterozoic and early Paleozoic rocks of the map area make up a portion of the core and eastern, upright limb of the west-verging Blue Ridge anticlinorium, a structure

formed during one or more compressional tectonic events in the middle to late Paleozoic. The formation of this large structure was accompanied by the development of at least two sets of cleavage, several generations of folds, minor local thrust and normal faults, and perhaps major underlying thrust faults not exposed in the map area. Deformation occurred under greenschist-facies metamorphic conditions, at chlorite or biotite grade, which has resulted in substantial recrystallization of these rocks and formation of Paleozoic mineral assemblages.  $^{40}\text{Ar}/^{39}\text{Ar}$  dating of metamorphic muscovite from early-developed cleavage in these rocks has set a probable age for deformation in this region as late Paleozoic (Burton and others, 1992a; Kunk and others, 1993).

#### FIRST-GENERATION PALEOZOIC CLEAVAGE

The most pervasive manifestation of Paleozoic deformation in the Blue Ridge anticlinorium is the development of a closely spaced cleavage or schistosity in both basement and cover-sequence rocks that accompanied a weak to strong metamorphic recrystallization. The first-generation schistosity, or  $S_1$ , is northeast striking and moderately to gently east dipping (fig. 12A), roughly parallel to the axial plane of the anticlinorium. The small scatter of data in figure 12A illustrates the uniformity of the  $S_1$  cleavage in all rock units.

In the Middle Proterozoic basement gneisses,  $S_1$  is commonly the dominant fabric in the rock, overprinting and obscuring the Middle Proterozoic foliation and layering. Formation of  $S_1$  was accompanied by the breakdown of older high-grade minerals and the growth of muscovite, chlorite, and (or) biotite along foliation planes, along with epidote and other greenschist-facies minerals. A steeply southeast plunging mineral lineation, typically composed of biotite or chlorite, is locally visible on the  $S_1$  surface. The lineation may in some cases represent the intersection of Middle Proterozoic foliation (or lineation) and Paleozoic schistosity or alternatively may indicate slip direction during noncoaxial compression and shear along the  $S_1$  plane.

“Ductile deformation zones” or DDZ’s, which consist of outcrop-scale, complex anastomosing networks of small faults and shear zones in flat “pavement” outcrops of basement rock, were described by Mitra (1979) and Boyer and Mitra (1988) in areas farther south in the Blue Ridge anticlinorium. In these areas the regional cleavage in the Blue Ridge anticlinorium (“Blue Ridge–South Mountain cleavage”) is, according to them, represented by the acute bisectrix of these anastomosing shear zones. DDZ’s are rare in the field area, perhaps partly due to the paucity of pavement outcrop. In any case,  $S_1$  in the map area has a much more planar fabric than that described for the DDZ’s.

In the metadiabase dikes of the basement and the lithologically similar metabasalts of the Catocin Formation,

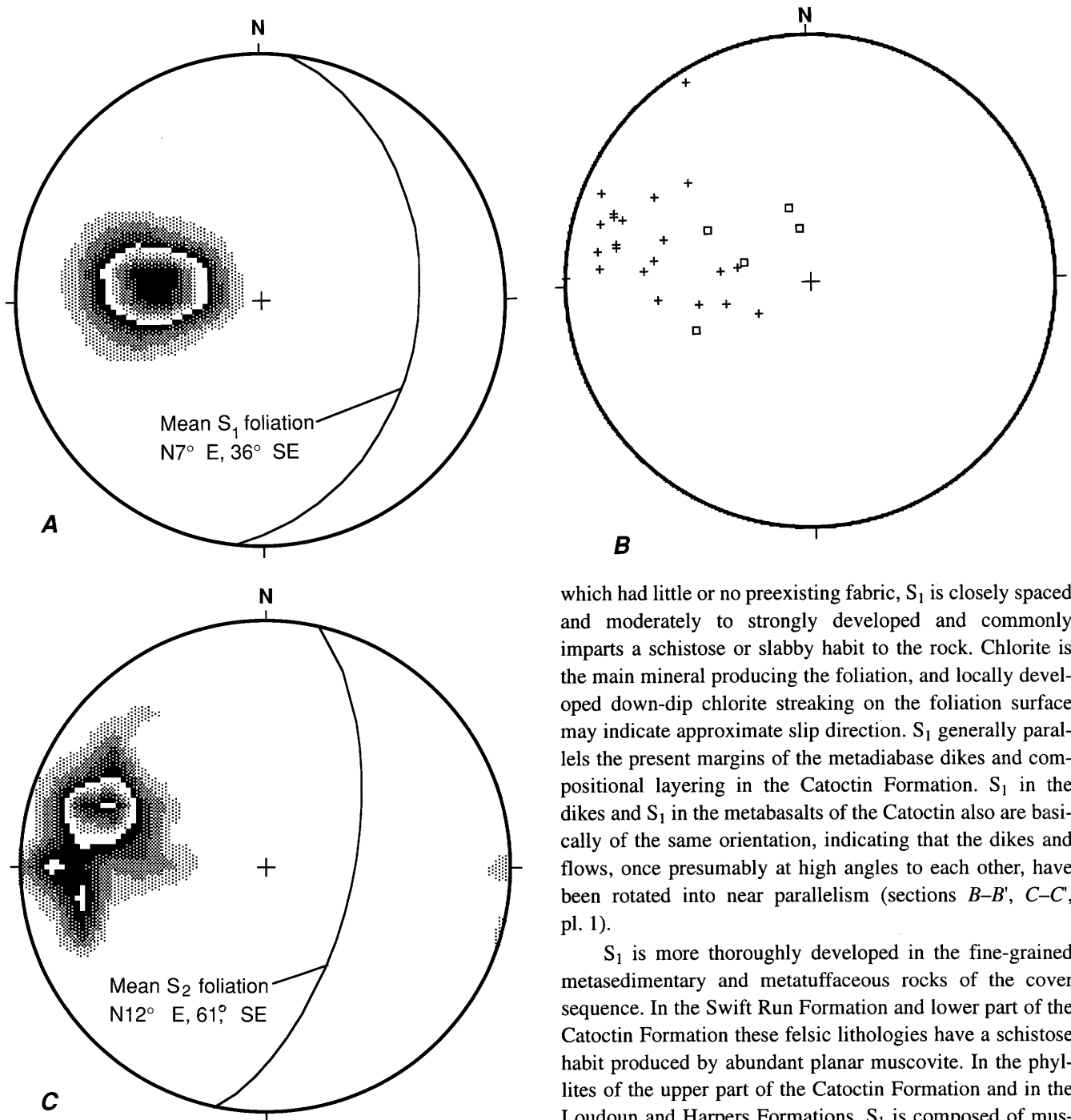


**Figure 12.** Lower hemisphere equal-area projections of first- and second-generation structures of Paleozoic age; contour interval is 2 percent per 1 percent area. A, Poles to  $S_1$  foliation and mean  $S_1$  foliation ( $n=1017$ ). B, Poles to axial planes of  $F_1$  folds ( $\square$ ,  $n=5$ ) and  $F_2$  folds ( $+$ ,  $n=22$ ). C, Poles to  $S_2$  foliation and mean  $S_2$  foliation ( $n=71$ ).

which had little or no preexisting fabric,  $S_1$  is closely spaced and moderately to strongly developed and commonly imparts a schistose or slabby habit to the rock. Chlorite is the main mineral producing the foliation, and locally developed down-dip chlorite streaking on the foliation surface may indicate approximate slip direction.  $S_1$  generally parallels the present margins of the metadiabase dikes and compositional layering in the Catoctin Formation.  $S_1$  in the dikes and  $S_1$  in the metabasalts of the Catoctin also are basically of the same orientation, indicating that the dikes and flows, once presumably at high angles to each other, have been rotated into near parallelism (sections  $B-B'$ ,  $C-C'$ , pl. 1).

$S_1$  is more thoroughly developed in the fine-grained metasedimentary and metatuffaceous rocks of the cover sequence. In the Swift Run Formation and lower part of the Catoctin Formation these felsic lithologies have a schistose habit produced by abundant planar muscovite. In the phyllites of the upper part of the Catoctin Formation and in the Loudoun and Harpers Formations,  $S_1$  is composed of muscovite, biotite, chlorite, and (or) graphite and commonly parallels a fine compositional layering (figs. 10, 11).

In the more quartzofeldspathic metasediments, particularly those of the Loudoun Formation and Weverton Quartzite,  $S_1$  can be seen distinct from and at an angle to bedding. It most commonly strikes parallel to bedding and has a steeper east dip, as would be expected on the normal limb of a major west-verging fold. Cleavage density and dip angles change with lithologic transition from quartzitic (steeper, widely spaced) to phyllitic (shallower, closely spaced) layers.

### FIRST-GENERATION FOLDS

The structures identified as  $S_1$  on the map (pl. 1) are axial planar to rare isoclinal first-generation folds ( $F_1$ ) (fig. 12B). Outcrop-scale  $F_1$  folds are best seen in the Loudoun Formation and Weverton Quartzite at the northern end of Catoctin Mountain, along with their axial planar ( $S_1$ ) cleavage (fig. 9). Recumbent, isoclinal  $F_1$  folds are also well displayed in the lower part of the Catoctin Formation in thin metasedimentary layers intercalated with the metabasalt. Cryptic, larger isoclinal  $F_1$  folds in the Weverton Quartzite are implied by the presence of overturned crossbeds in some of the quartzite layers.  $F_1$  fold hinges are subhorizontal and generally strike northeast-southwest, parallel to the long axis of the Blue Ridge anticlinorium. The anticlinorium may itself be an  $F_1$  megafold and  $S_1$  its associated axial planar schistosity (Mitra and Elliott, 1980).  $S_1$  is the "Blue Ridge–South Mountain cleavage" of Mitra and Elliott (1980).

### SECOND-GENERATION CLEAVAGE AND FOLDS

Second-generation cleavage and schistosity ( $S_2$ ) is widespread but only locally developed in both basement and cover rocks. It is typically a spaced (1 cm or more) cleavage that cuts  $S_1$  schistosity, is approximately parallel to it in strike, and dips more steeply eastward (fig. 12C). In the map area,  $S_2$  is generally not accompanied by extensive recrystallization except at the northern end of Catoctin Mountain, where second-generation cleavage and folds are intensely developed. The roadcut of phyllite of the Loudoun Formation on U.S. Route 15 features a well-developed, penetrative schistosity of  $S_2$  generation.

$S_2$  cleavage is typically axial planar to second-generation ( $F_2$ ) folds.  $F_2$  folds generally have subhorizontal, north-east-striking hinges and gently to moderately east dipping axial surfaces (fig. 12B).  $F_2$  folds are rarely seen in the basement as mesoscopic folds of  $S_1$  schistosity in Middle Proterozoic gneiss or Late Proterozoic intrusive dikes. They also are found locally in greenstones in the lower part of the Catoctin Formation as closely spaced similar folds deforming  $S_1$ .

$F_2$  folds are most strongly developed and best exposed along the eastern limb of the anticlinorium in the uppermost part of the Catoctin Formation and lowermost part of the Chilhowee Group rocks (fig. 9), and they are a dominant factor in the map pattern of the northern end of Catoctin Mountain in Virginia. Here occurs an isolated inlier of Weverton Quartzite, which contrasts structurally with the continuous east-dipping section found along most of the limb. Whittaker (1955) inferred a fault to explain the disconnected quartzite; it is in fact the hinge of a large, shallow  $F_2$  syncline (Catoctin Mountain syncline), which has probably overprinted smaller  $F_1$  structures (section  $B-B'$ , pl. 1). The inlier of Tomstown Dolomite ( $\epsilon t$ ) and carbonaceous

phyllite ( $\epsilon cp$ ) west of Furnace Mountain is also interpreted as the hinge of an  $F_2$  syncline that was later cut by an early Mesozoic normal fault (Furnace Mountain fault) and that lies west of a complex (later overprinted)  $F_2$  anticline (Furnace Mountain anticline). Outcrop-scale, large-amplitude  $F_2$  folds are well displayed in well-foliated ( $S_1$ ) greenstone of the Catoctin Formation just west of U.S. Route 15, and are sufficiently developed to generate a locally pervasive  $S_2$  schistosity in phyllite of the Loudoun Formation, as mentioned above. From west to east in this small area, the axial surfaces of these folds appear to rotate from steeply to moderately east dipping, perhaps in response to later folding or as a result of fanning cleavage.  $F_2$  folds in thin phyllitic layers in the Weverton Quartzite just above its contact with the Loudoun Formation produce a closely spaced crenulation cleavage axial planar to the folds. Farther south along Catoctin Mountain,  $F_2$  folding is less pervasive but probably responsible for local dip reversals in  $S_1$  in the Catoctin Formation and Weverton Quartzite.

Second-generation folds also are found locally on the western limb of the anticlinorium, such as at Purcell Knob (Nickelsen, 1956; Southworth, 1991). In the anticlinorium as a whole, second-generation  $F_2$  folds probably occur as minor, local modifications of the major  $F_1$  structure.

### LATE FOLDS

Folds that postdate  $F_1$  and  $F_2$  folds are locally well developed in the cover sequence and rarely occur in basement rocks. These can be divided into two types based on fold style: low-amplitude and short-wavelength (few millimeters to centimeters) crenulate or kink folds (figs. 10, 13A) and larger (up to 1–2 m in amplitude and wavelength) open to isoclinal cylindrical folds (fig. 13B).

Planar kink folds and minor crenulations are found in phyllitic cover-sequence rocks and schistose rocks of the basement. They all have subhorizontal hinges but can be divided into three sets based on axial surface orientation: a north-trending set having steep east or west dips; a north-west-trending set, also having steep dips; and a minor set having gentle to moderate dips (and one steep dip) and widely varying strikes (fig. 13A). These minor folds are particularly prominent along the northeastern side of Catoctin Mountain in the phyllites of the Loudoun and Harpers Formations (fig. 10). Steeply to moderately west dipping crenulations are locally associated with minor east-verging back thrusts that have as much as 1 cm of offset. These kink or crenulation folds may represent the last stages of compression in the stress field that produced the structure of the Blue Ridge anticlinorium; the back thrusts represent a final strain-induced response to the buttressing effect of the already formed anticlinorium.

Rare late cross folds generally have shallow- to moderate-plunging hinges and northeast or northwest axial

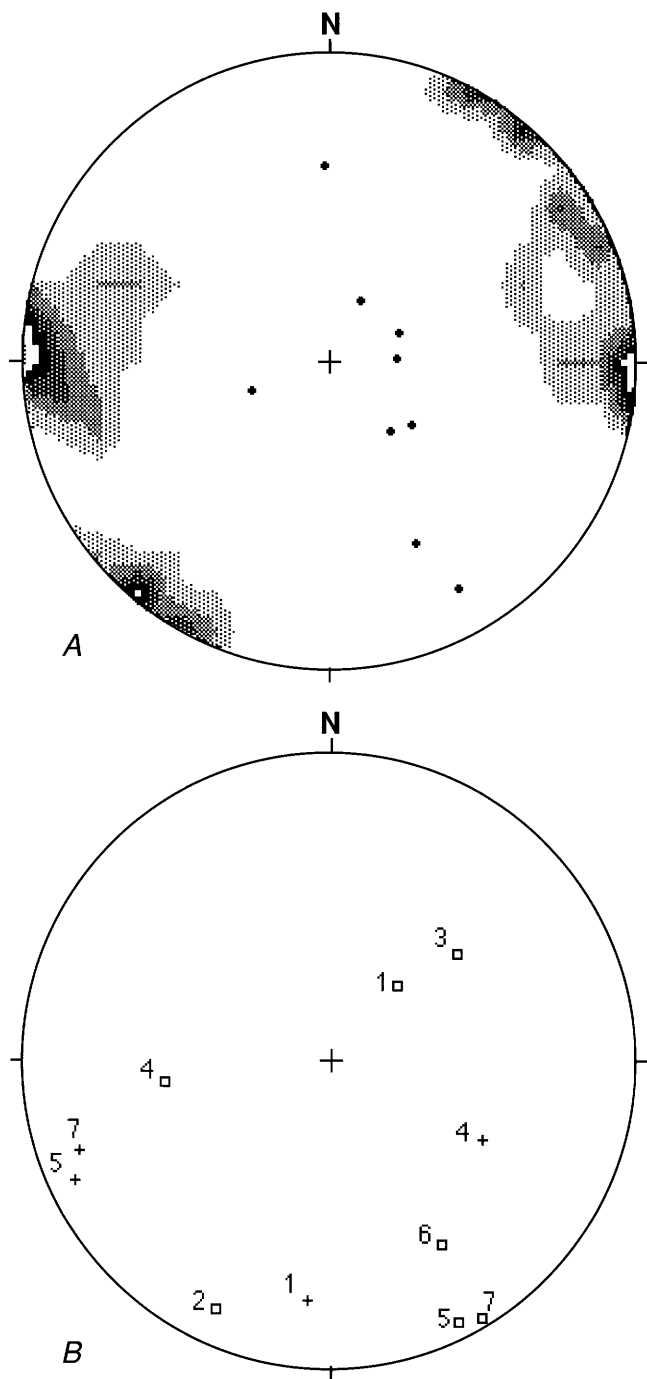


**Figure 13.** Lower hemisphere equal-area projections of late folds. *A*, Contoured poles to steeply dipping late crenulate cleavage or steeply dipping axial planes of crenulate folds; contour interval is 2 percent per 1 percent area ( $n=35$ ); poles to gently dipping cleavage or axial planes of crenulate folds ( $\bullet$ ,  $n=9$ ). *B*, Poles to axial planes of late cross folds ( $\square$ ,  $n=7$ ) and hinges of late cross folds, where measurable ( $+$ ,  $n=4$ ). 1, meter-scale, east-verging recumbent fold in Frederick Limestone ( $\epsilon_f$ ); 2, 3, open folds in Weverton Quartzite ( $\epsilon_w$ ); 4, meter-scale recumbent fold in Catoctin Formation ( $Z_c$ ); 5, 6, 7, open folds in Tomstown Dolomite.

planar trends (fig. 13*B*). They have a different geometry from the kink folds, as mentioned above. These cross folds were found only in Catoctin Formation, Weverton Quartzite, and Tomstown Dolomite on or east of Catoctin Mountain (fig. 13*B*). The tectonic significance of these folds is poorly understood; one observed fold in Frederick Limestone is east verging (no. 1 in fig. 13*B*). In the carbonate rocks, interaction between cross folds of several orientations has produced complex interference patterns in outcrop. On a larger scale, the complex map pattern produced by the Harpers Formation, Antietam Quartzite, and the carbonates around Furnace Mountain is interpreted to be the product of these interfering cross folds superimposed on older, larger amplitude folds such as the Furnace Mountain ( $F_2$ ) anticline. The cross folds are perhaps a product of late Alleghanian dextral transcurrent motion that has been documented elsewhere (Gates and others, 1986).

#### THE TECTONIC ROLE OF FAULTING

On a large scale, the structures of the Blue Ridge are considered by many workers to be ultimately derived from low-angle, east-over-west thrusting (Harris, 1979; Mitra and Lukert, 1982; Evans, 1989). In this study, convincing evidence for or against large-scale thrusting was not found. A few mylonite zones were mapped in the basement of which two, as discussed above, have kinematic indicators showing a normal (east side down) sense of movement (sections A-A', C-C', pl. 1). A third has features showing an east-over-west sense of movement (section C-C') and is probably coeval with Blue Ridge compressional events. All mapped faults, however, are minor in extent and probable degree of offset; strain accommodation during formation of the Blue Ridge anticlinorium, in this small area at least, was by the more ductile processes of folding and cleavage development. The model developed by Mitra and Lukert (1982) of a single, fanning generation of cleavage (Blue Ridge-South Mountain cleavage) linked to an episode of deep-seated thrusting may apply to  $S_1$  but does not explain the two overlapping generations of cleavage here ( $S_1$  and  $S_2$ ) nor the several late generations of folds.

#### LATE BRITTLE STRUCTURES

The youngest tectonic structures of possible Paleozoic age in the Blue Ridge anticlinorium are joints and brittle faults. The joints typically have steep dips but no strong preferred azimuth (fig. 14*A*). A Mesozoic or younger age for these structures also cannot be ruled out, as there is significant overlap in orientation between joints in pre-Mesozoic and Mesozoic rocks (figs. 14*A*, 15). However, the north-northeast and south-southwest pole concentrations in the pre-Mesozoic rocks (fig. 14*A*) are absent from the plot of Mesozoic joints (fig. 15); these pole concentrations, at

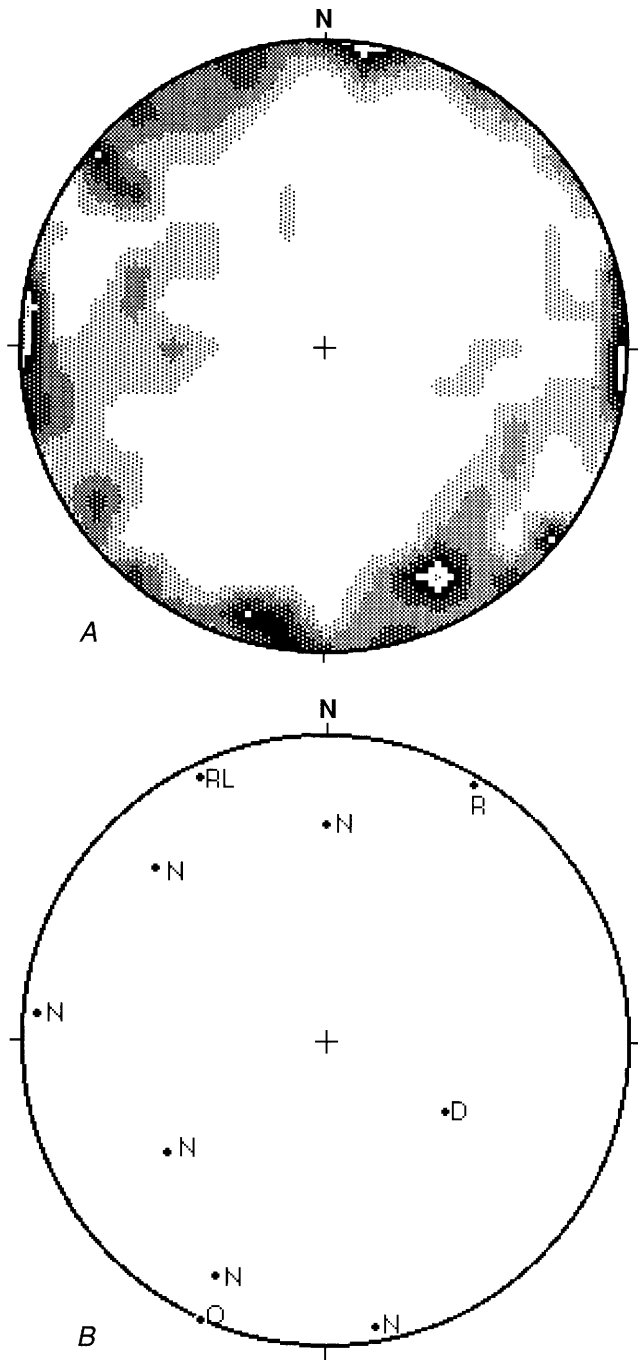


**Figure 14.** Lower hemisphere equal-area projections of late brittle structures in pre-Mesozoic rocks. *A*, Poles to joints; contour interval is 1 percent per 1 percent area, ( $n=80$ ). *B*, Poles to faults with outcrop scale offset or slickenlines; letter indicates apparent movement sense: N, normal; R, reverse; RL, right lateral; D, dip slip; O, oblique slip.

least, can be more confidently assigned a Paleozoic age. A number of brittle faults measured in outcrop have offsets of a few centimeters or slickenlines indicating slip direction (fig. 14*B*). These show no consistent preferred orientation.

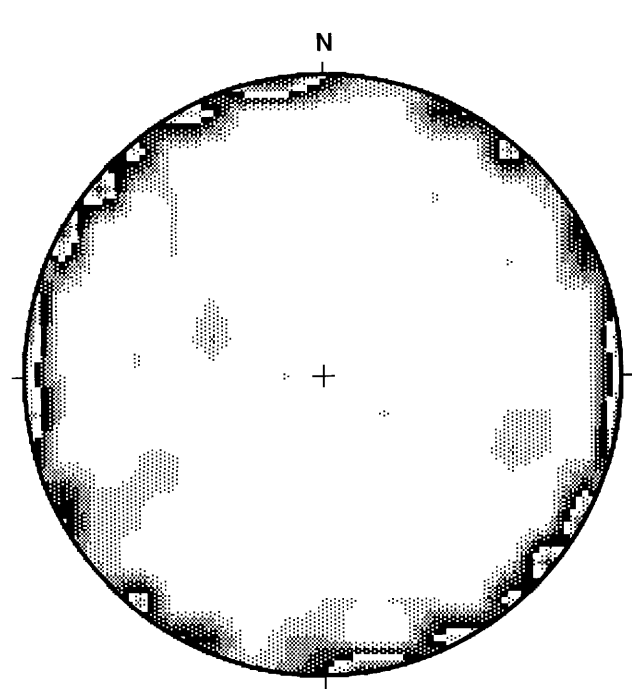


**Figure 15.** Lower hemisphere equal-area projection showing contoured poles to joints in the Culpeper basin; contour interval is 1 percent per 1 percent area ( $n=94$ ).

#### PALEOZOIC RECRYSTALLIZATION AND METAMORPHIC GRADE

The Paleozoic deformation of the rocks in the northern Blue Ridge was accompanied by recrystallization under greenschist-facies conditions. In pelitic rocks, such as those of the Harpers Formation, this metamorphism produced widespread biotite but no garnet (fig. 11). In some rocks, metamorphic recrystallization began before principal deformation ( $S_1$ ,  $F_1$ ) as well as accompanying and following it.

Recrystallization in the Middle Proterozoic gneisses produced low-grade mineral assemblages that are in sharp contrast to the original high-grade assemblages of the gneisses. In the granitic rocks, Paleozoic muscovite, chlorite, epidote, and secondary greenish biotite grew at the expense of feldspar and primary brown biotite, primarily during development of the  $S_1$  schistosity. Garnet in the rusty paragneiss (Yrg) is largely chloritized, and the mafic minerals in the hornblende-pyroxene gneiss are uralitized or extensively altered to actinolite and chlorite. In all of these rocks, plagioclase has cloudy overgrowths of sericite and saussurite and is now albite in composition. Quartz commonly has undulatory extinction or has recrystallized into a fine-grained mosaic. Biotite and muscovite grew in the mylonitic foliation of shear zones in the basement, indicating that the metamorphic age of these zones is compatible with Paleozoic deformation.

The greenstones of the Late Proterozoic mafic dikes and the metabasalts of the Catocin Formation have typical

mafic greenschist-facies mineral assemblages, including actinolite, chlorite, and epidote. Muscovite, derived from plagioclase, is also common, and minor amounts of greenish-brown biotite may be present. Metamorphic recrystallization appears to have begun before and continued during development of foliation. In the coarser grained, actinolite-bearing diabase dikes (Zda) and actinolitic greenstones of the Catoctin (Zca), prekinematic amphibole growth is shown by stubby crystals of pale-green actinolite, presumably pseudomorphs developed from igneous clinopyroxene during the early stages of metamorphism, that have rims that have broken down into foliation-parallel chlorite. In the fine-grained greenstones, particularly the metabasalts of the Catoctin, small blue-green actinolite laths have grown in the plane of the  $S_1$  foliation, indicating amphibole growth that is synkinematic with respect to  $S_1$ .

In the pelitic rocks such as the Harpers Formation phyllite, muscovite, biotite, and to a lesser extent chlorite are well developed and define the foliation. No garnet has been found, even in the easternmost rocks, where metamorphic grade might be higher.  $F_1$  and  $F_2$  folding both occurred under peak biotite-zone conditions, whereas in the noses of the later crenulations and cross folds biotite is partially retrograded to chlorite. Only the late brittle structures such as joints and microfaults, some of which may be younger than Paleozoic, appear to be postmetamorphic in age.

#### $^{40}\text{Ar}/^{39}\text{Ar}$ DATING OF METAMORPHIC FABRIC

Muscovite that defines the dominant foliation in several units in the cover-sequence rocks has been sampled, and three of these samples were analyzed by the  $^{40}\text{Ar}/^{39}\text{Ar}$  age-spectrum technique to determine the age of the foliation and timing of Paleozoic deformation. The rock units sampled (from west to east) were fine-grained tuffaceous quartz-muscovite phyllite in the lower part of the Catoctin Formation (Zct), strongly cleaved Weverton Quartzite ( $\epsilon w$ ) on the western (overturned) limb of the Catoctin syncline, and Loudoun Formation phyllite ( $\epsilon l$ ) from the roadcut on U.S. Route 15 (black diamond symbol, pl. 1). The schistosity in the tuffaceous schist and Weverton Quartzite is mapped as  $S_1$ , and the muscovitic cleavage in the quartzite is axial planar in outcrop to a mesoscopic  $F_1$  fold. The dominant schistosity in the phyllite on U.S. Route 15 is mapped as  $S_2$ , with earlier,  $S_1$ , fabric being completely transposed.

These samples yield complex spectra that do not have plateaus and do not yield precise estimates of the timing of muscovite growth (Burton and others, 1992a; Kunk and others, 1993). This suggests that the muscovite is of multiple generations, although petrographic evidence indicates a single, dominant generation of cleavage-producing mica; apparently there was some fine-grained muscovite growth or recrystallization at temperatures below the argon closure temperature for muscovite ( $\sim 350^\circ\text{C}$ ) (Kunk and others,

1993). Despite the difficulty of interpretation, these data and other data to the south suggest a late Paleozoic age (350–300 Ma) for the development of the regional ( $S_1$ ) cleavage and seem to rule out a pervasive early Paleozoic (Taconian) metamorphic event (Burton and others, 1992a).

## GEOLOGY OF EARLY MESOZOIC ROCKS

The eastern half of the map area is underlain largely by Upper Triassic sedimentary rocks of the Culpeper Group of the Newark Supergroup and by minor areas of Early Jurassic diabase in the early Mesozoic Culpeper basin. The sedimentary rocks, from base to top, consist of pink to gray arkosic sandstone and red-brown siltstone of the Poolesville Member of the Manassas Sandstone, conformably overlain by dark-red Balls Bluff Siltstone, which grades laterally into and is locally overlain by light-gray limestone conglomerate lentils of its Leesburg Member. No diagnostic fossils have been found in these rocks within the map area; however, correlative beds in the Balls Bluff Siltstone nearby have been dated as Late Triassic on the basis of palynomorphs (Cornet, 1977). These strata are locally intruded by dark-gray diabase dikes and sheets that have been dated nearby as Early Jurassic (Sutter, 1985, 1988). Similar diabase dikes also intrude the pre-Mesozoic crystalline rocks west of the basin, one of which also yields an Early Jurassic age (Kunk and others, 1992). The Triassic sedimentary rocks regionally dip westward at moderate to gentle angles, are inferred to be cut by poorly exposed, northeast- and northwest-striking normal faults, and are separated from the Lower Paleozoic rocks to the west by a major normal border fault, the Bull Run fault of Roberts (1923).

## SEDIMENTARY ROCKS

### MANASSAS SANDSTONE, POOLESVILLE MEMBER

The stratigraphically lowest Mesozoic unit within the map area is the Poolesville Member of the Manassas Sandstone ( $\epsilon mp$ ), which consists of pinkish-gray to reddish-brown sandstone and reddish-brown siltstone that occur in upward-fining sequences 3 to 6 m thick. The sandstone is fine- to coarse-grained, locally pebbly, arkosic, micaceous, ferruginous, and locally silty and calcareous. It consists chiefly of subrounded and subangular quartz and feldspar grains in a ferruginous, micaceous, silty clay matrix cemented by clay, iron oxide, silica, and calcite. It is thin- to thick bedded and massive and is both planar and crossbedded, especially in pebbly channel-fill sequences where angular red shale chips are locally common. Dusky-red to reddish-brown siltstone and silty and sandy shale form the top of the upward-fining units. Only the uppermost 105 m of the thick-bedded sandstone crops out along the northeastern margin of the quadrangle; it is poorly exposed and

deeply weathered on upland surfaces. The Poolesville Member is conformably and gradationally overlain by the Balls Bluff Siltstone. Although the base of the formation is not exposed in the map area, in adjacent areas it overlies a basal carbonate conglomerate member that is unconformable on Paleozoic carbonates (Lee and Froelich, 1989).

#### BALLS BLUFF SILTSTONE AND ITS LEESBURG MEMBER

This unit (Fb) consists of dusky-red to reddish-brown siltstone, sandstone, mudstone, and shale, which are interbedded in upward-fining sequences. The siltstone is mainly dusky red, reddish brown, dark red, and grayish red, micaceous, feldspathic, ferruginous, clayey, sandy, and calcareous; carbonate nodules (caliche) and calcite veinlets are locally common. It is thin bedded to massive and commonly bioturbated (mainly by rootlets) and has irregular bedding and hackly fractures. Reddish-brown, fine-grained sandstone that grades upward into climbing-ripple, cross-laminated, sandy siltstone is common near the base of the unit, and lenticular layers of dusky-red, silty and sandy calcareous shale are common throughout the sequence. Where the poorly exposed sandy siltstone intertongues with the carbonate conglomerates of the Leesburg Member (Fb1), the latter commonly forms low strike ridges that are prominent to the southeast but generally die out to the northwest. The lower fluvial siltstones of the Balls Bluff overlie the Poolesville Member of the Manassas Sandstone conformably and gradationally along the eastern margin of the quadrangle. Siltstones of the main mass of Balls Bluff intertongue extensively with the alluvial fan conglomerates of the Leesburg Member to the northwest; therefore much of the estimated thickness of 1,200 m is applicable to the conglomerates as well. The Balls Bluff Siltstone is well exposed at the type locality along the bluffs of the Potomac River near Balls Bluff National Cemetery where Lee (1977) described his partially measured section 6. Farther north and west, the siltstone is deeply weathered and mantled on upland surfaces by leached, micaceous residuum as much as 6 m thick. Although no diagnostic fossils have been found in these beds in the map area, the upper part of the Balls Bluff Siltstone in nearby areas (lacustrine member) has been dated as Late Triassic (probably Norian) on the basis of palynomorphs in gray siltstone (Lee and Froelich, 1989).

The Leesburg Member (Fb1) of the Balls Bluff Siltstone is chiefly limestone and dolostone conglomerate that contains minor partings and lenticular intercalations of calcareous sandstone and siltstone and a friable, coarse-grained, pebbly, arkosic sandstone at the base in the northern part of the area. In weathered outcrops the conglomerate is light gray, and the varicolored clasts give it a conspicuous mottled appearance. On fresh surfaces it consists mainly of subangular to subrounded boulders, cobbles, and pebbles of light-gray to grayish-black and pinkish-red clasts of

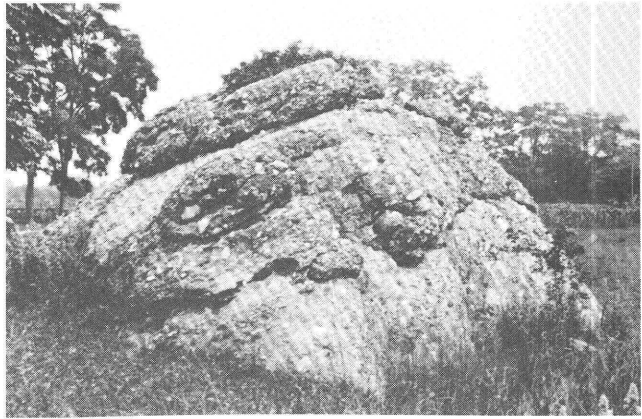


**Figure 16.** Outcrop of carbonate conglomerate, Leesburg Member of Balls Bluff Siltstone, just west of junction of State Routes 661 and 15. Outcrop is about 4 m across.

Cambrian and Ordovician limestone and dolomite embedded in a variable matrix of calcareous reddish-brown gravel, sand, or clayey silt. The conglomerate contains minor clasts of quartzite, vein quartz, chert, marble, phyllite, slate, and greenstone, but more than 95 percent of the clasts are laminated to massive carbonate (Hazlett, 1978; Lindholm and others, 1979).

The conglomerate is thick bedded to massive; beds average 3 m in thickness (fig. 16). These beds are commonly lenticular where defined by alternations of red muddy matrix-supported conglomerates and clast-supported conglomerates having well-rounded pebble layers and matrix- and calcite-cement-filled interstices. Measured section 7 of Lee (1977) includes the type section of the Leesburg Member, which is exposed in roadcuts southeast of the junction of U.S. Route 15 bypass and the entrance road to Balls Bluff National Cemetery. A more detailed description of the variety of conglomerate fabrics near the type section and interpretations of their possible origin as debris flow and shallow sheetflood or flashflood deposits on an alluvial fan can be found in field trip no. 3, stop 4, in the Geologic Society of America Guidebook (p. 67–69 in Froelich and others, 1982). Rock fragments in the conglomerate generally increase in size northwesterly; cobbles that average about 6.35 cm in diameter near the type section increase to as large as 1.2 m near Limestone Branch about 3.2 km to the north. In places the conglomerate layers are interbedded with 0.3- to 3.0-m-thick layers or lenses of red calcareous pebbly sandstone, calcareous sandy siltstone, and red-brown massive mudstone that are progressively thicker to the south and east where they tongue into the main body of Balls Bluff Siltstone (Fb).

The conglomerate apparently occurs in lobate deposits that overlap stratigraphically, although some conglomerate lentils are separated by red-brown sandstone and siltstone

sequences. Hazlett (1978) has shown that the stratigraphically lowest lobes (most northerly and easterly) predominantly are composed of dolostone clasts, whereas the stratigraphically highest lobes (most southwesterly) mainly are composed of limestone clasts. In the northern part of the map area, the lowest dolostone conglomerate is underlain by a distinctive, friable, pebbly arkose that appears to be disconformable on the underlying siltstone. The Leesburg Member is fairly well to poorly exposed; commonly low, rounded strike ridges of bare, pitted conglomerate can be traced continuously for about 100 m and discontinuously for about 0.5 km (fig. 16). Such low ridges are separated by subdued parallel valleys and are underlain in places by deeply and irregularly weathered limestone conglomerate pinnacles mantled by as much as 10 m of noncalcareous, dark-red, clay- and silt-rich residuum (*terra rosa*); elsewhere the strike valleys are developed on intercalations of friable, calcareous, red-brown sandstone and siltstone. In many places on the carbonate conglomerate landscape, characteristics typical of karst or karren country are developed, such as sinkholes, caves, overhangs, solution pits, disappearing streams, tufa deposits, and springs (discussed below). The sinkholes, solution pits, tufa deposits, and springs are shown on plate 1.

The Leesburg Member conformably overlies the lower fluvial siltstones of the Balls Bluff Siltstone (Fb) and tongues into and is laterally gradational to the main body of siltstone to the southeast. Lee (1977) has calculated the thickness of the Leesburg Member in this area as 3,510 ft. However the carbonate conglomerate lentils overlap stratigraphically, are cut by faults, thin and pinch out into Balls Bluff Siltstone to the southeast, and are truncated by the border fault on the west; therefore it is unlikely that this composite thickness is representative.

## IGNEOUS AND METAMORPHIC ROCKS

### DIABASE

The Upper Triassic sedimentary rocks of the Culpeper basin and the pre-Mesozoic rocks to the west are intruded by diabase dikes and plugs of Early Jurassic age. In most cases the dikes are poorly exposed and are known only from linear arrays of spheroidal boulders embedded in residual saprolite and soils, which weather a distinctive orange. Where fresh the diabase is medium to dark gray and chiefly medium grained and equigranular, but it is fine grained and aphanitic near chilled margins and in narrow dikes. Compositionally, the diabase is a quartz-normative tholeiite of at least two magma types: (1) low-TiO<sub>2</sub> quartz normative (Jdl) and (2) high-TiO<sub>2</sub> quartz normative (Jdh) (LTQ and HTQ magmas, respectively, of Weigand and Ragland, 1970). Minor diabase dikes of undetermined compositions are shown on plate 1 as Jd, including most of the dikes mapped in the pre-Mesozoic rocks. As no direct age determinations

**Table 4.** Major oxide geochemistry (weight percent) of high-titanium, quartz-normative Jurassic diabase dike (Jdh), Waterford quadrangle.

[Ten-element ICP analysis by Hiram Smith; total iron as Fe<sub>2</sub>O<sub>3</sub>]

| Major oxide                    | Sample<br>Map unit<br>Sample site |
|--------------------------------|-----------------------------------|
|                                | AJF-91-Wat-1<br>Jdh<br>17         |
| SiO <sub>2</sub>               | 51.3                              |
| Al <sub>2</sub> O <sub>3</sub> | 13.8                              |
| Fe <sub>2</sub> O <sub>3</sub> | 11.3                              |
| MgO                            | 7.6                               |
| CaO                            | 10.4                              |
| Na <sub>2</sub> O              | 1.9                               |
| K <sub>2</sub> O               | .46                               |
| TiO <sub>2</sub>               | 1.1                               |
| P <sub>2</sub> O <sub>5</sub>  | .16                               |
| MnO                            | .2                                |
| Loss on ignition               | 1.72                              |
| Total                          | 99.94                             |

were made, the inferred Early Jurassic age is based on <sup>40</sup>Ar/<sup>39</sup>Ar age spectrum dates from similar diabase elsewhere in the Culpeper basin (Kunk and others, 1992; Sutter, 1985, 1988).

Texturally, LTQ diabase (Jdl, pl. 1) is characterized by widely scattered centimeter-sized phenocrystic clusters of calcic plagioclase (chiefly labradorite) embedded in generally aphyric diabase. The diabase is composed of an interlocking crystalline mosaic of fine, equigranular pyroxene (mainly augite), euhedral laths of fine-grained groundmass plagioclase, and minor amounts of interstitial oxides (mostly magnetite) and sulfides. In the map area, LTQ diabase occurs as a northeast-striking dike about 25 m wide intruding siltstone near the Potomac River about 4 km southeast of Lucketts, as a northwest-striking narrow dike intruding sandstone about 3.8 km northeast of Lucketts, and as a narrow, north-striking dike cutting the crystalline rocks of Catocin Mountain about 4 km northwest of Lucketts. Elsewhere, minor spheroidal boulder debris may indicate the presence of other narrow dikes, as near State Route 658 about 4.3 km north-northeast of Lucketts.

HTQ diabase (Jdh, pl. 1) consists mainly of medium-grained, interlocking crystals of pyroxene (mainly augite) and euhedral laths of plagioclase and minor amounts of interstitial oxides (magnetite and ilmenite). It is generally aphyric but locally aphanitic at chilled margins and where dikes are thin. HTQ diabase occurs as an irregularly shaped (inverted V) sheet or plug, about 900 m wide and possibly as much as 150 m thick, that intrudes siltstone and limestone conglomerate about 1.6 km northeast of Lucketts. Major oxide geochemistry from a sample of this body (no. 17 on pl. 1) indicates that it is a quartz-normative tholeiite (table 4).

### THEMALLY METAMORPHOSED ROCKS

Hornfels, meta-arkose, and marble occur in zoned contact aureoles (Jtm) adjacent to diabase bodies. The hornfels is gray, dark gray, bluish gray, and mauve, and the meta-arkose is commonly pink or light gray. Cordierite pseudomorphs and biotite crystals are common in the inner aureole, and epidote and chlorite occur in the outer aureole. The marble, derived from clasts in the carbonate conglomerate (Fbl), is gray to light gray and contains coarse calcite and minor amounts of grossularite, diopside, and wollastonite locally developed (Lee, 1982; Lee and Froelich, 1989). The thermal aureole surrounding the thickest part of the HTQ diabase sheet or plug northeast of Lucketts may be as much as 30 m thick, but in most areas the aureole is less than 6 m thick. The hornfels and meta-arkose are hard, brittle, and fractured but do not weather readily; bedrock is thus generally shallow; soil and saprolite are less than 1 m thick. The fractured marble, however, weathers readily and is rarely exposed. It is generally only seen as angular blocks and fragments in soil and as leached and weathered material more than 6 m thick.

### STRUCTURAL GEOLOGY

The structure of the Culpeper basin in the map area can be characterized generally as consisting of sedimentary beds dipping homoclinally westward towards a north- to northeast-striking, east-dipping, normal border fault, the Bull Run fault of Roberts (1923). The Triassic sedimentary rocks generally strike northerly and dip moderately to gently westward at 10 to 35 degrees. The orientation of the strata combined with the strike of the fault result in progressively lower Triassic strata being truncated by the fault in a northward direction. The Triassic strata are warped gently into broad, probably faulted flexures, most notably the south-plunging Morven Park syncline (pl. 1 and cross section *D-D'*) and a west-plunging anticlinal nose near Limestone Branch, and are also offset by inferred cross-basin faults that apparently define a series of graben and horsts.

#### BULL RUN FAULT

The Bull Run fault (Roberts, 1923) is the normal border fault that marks the western margin of the Culpeper basin in the map area. This fault extends north-northeasterly along the eastern flank of Catocin and Bull Run Mountain. In the southern part of the map it borders the Weverton Quartzite, whereas to the north the fault truncates progressively younger pre-Mesozoic units. North of U.S. Route 15 near the Potomac River, a splay of the border fault extends sharply eastward and then northward again, separating the highly deformed Cambrian Frederick Limestone (€f) from the Triassic limestone conglomerate of the Leesburg Mem-

ber (Fbl). Another splay of the fault is inferred to continue straight northward parallel to the contact of Tomstown Dolomite (€t) and Frederick Limestone. The Bull Run fault is also responsible for a small wedge of downdropped Antietam Quartzite (€a) near the center of the Waterford quadrangle.

The border fault in this area is inferred to dip about 50 degrees eastward at the surface (sections *B-B'*, *C-C'*, *D-D'*, pl. 1), based on sparse excavation and well data from, and former exposures in, the Waterford quadrangle and the adjacent Leesburg quadrangle (Roberts, 1923). However, in Limestone Branch where the stream intersects the trace of the fault, the evidence suggests a locally shallower dip. Here the fault is at least partially exposed at the eastern end of a long continuous outcrop of Weverton Quartzite. From west to east, the fault zone exposure contains about a meter of greenish-gray to rusty-weathered, shallowly east-dipping foliated cataclasite, which is derived from the Weverton Quartzite (the footwall). The cataclasite is overlain to the east by about 3 m of massive, saprolitized, orange fault gouge containing irregular to planar dark-red hematite-rich zones near the contact with the cataclasite, followed eastward by bright red saprolite apparently derived from Balls Bluff Siltstone (hanging wall). The dip in the foliated cataclasite was measured as approximately 25 degrees. To the west this fault fabric disappears over a short distance (a few meters or so) within the main exposure of Weverton Quartzite.

An outcrop of cataclastic Weverton Quartzite about 50 m west of gently dipping Balls Bluff Siltstone can also be seen in a creek immediately north of State Route 698 at the northwestern corner of the town of Leesburg. Weak flexion structure in the cataclastic Weverton at one spot dips eastward at 45 degrees.

Most of the observable border-fault-related structures in the footwall of the Bull Run fault are complex and consist of a variably oriented, crisscrossing network of fine fractures, microfaults, and thin zones of microbreccia. These features disappear a few tens of meters from the fault. Mineralization associated with the fractures and microbreccia includes fine veins of quartz and calcite, hematite and carbonaceous material in the microbreccia zones, and minor sulfides and euhedral hematite crystals. Discontinuous, dark-red hematite-filled microfractures in white Weverton Quartzite adjacent to the border fault constitute the most commonly seen form of mineralization associated with the Mesozoic border fault in this area.

#### FURNACE MOUNTAIN FAULT AND RELATED FAULTS AND LINEAMENT

Two small faults extend northwest from the Bull Run fault north of State Route 663 and converge into the Furnace Mountain fault, which cuts north and crosses the Potomac River near the Point of Rocks bridge. The

northwest-striking faults downdrop a portion of the Antietam Quartzite, and one is continuous with a northwest-trending lineament that crosses the Culpeper basin (pl. 1). The latter feature is a conspicuous tonal lineament on aerial photos (Leavy, 1984) and radar imagery.

The best evidence for normal offset on the Furnace Mountain fault can be found in a creek just southwest of Furnace Mountain. Here an exposure of Tomstown Dolomite occurs only about 20 m east of an outcrop that is compositionally transitional between the Harpers Formation and the Antietam Quartzite and that passes westward (downward) into continuously exposed phyllite of the Harpers. The minimum fault offset here is thus inferred to be equal to the thickness of the Antietam, or about 100 ft; on section B-B' (pl. 1), about 450 m to the north, it is shown as about 250 ft. Farther north, near the river, the offset is greater, and the fault juxtaposes Catoctin Formation (Zc) and carbonaceous phyllite (Є<sub>cp</sub>). The Furnace Mountain fault crosses the river to Point of Rocks, Md., where it may account for the juxtaposition of the Harpers Formation and Tomstown Dolomite as mapped by Whittaker (1955).

#### INFERRED FAULTS

The Triassic sedimentary rocks of the Culpeper basin in the Waterford and Point of Rocks quadrangles are here interpreted to be cut into fault blocks by a series of inferred regional north-northeast-trending faults. Previously the mapped distribution of basin lithofacies (carbonate conglomerate, T<sub>1</sub>b<sub>1</sub>, and sandy siltstone and shale, T<sub>1</sub>b were interpreted to be the product of lateral facies changes (Lee and Froelich, 1989). However these facies changes are too abrupt when viewed in the context of feasible alluvial-fan depositional models (Smoot, 1991; J.P. Smoot, U.S. Geological Survey, written commun., 1991). The sharp lateral transition between thick sequences of conglomerate and adjacent sandy siltstone and shale are better explained by a faulted, graben and horst geometry. The inferred faults on plate 1 are projected from better exposed faults mapped to the northeast that cut and offset the pre-Mesozoic rocks along the scalloped northeastern margin of the Culpeper basin. Radar imagery and air photos of the map area show truncated features and subtle tonal changes across linear features coincident with some of the inferred faults. The inferred faults at and northeast of the junction of U.S. Route 15 and Business Route 15 are associated with a series of springs and tufa deposits (pl. 1).

#### RELATIVE TIMING OF MESOZOIC FAULTING

The timing of movement on the Mesozoic faults is not precisely known. No Jurassic diabase dikes have been observed cutting the faults, and no faulted dikes are known. Continued border fault movement in the Triassic is implied by the presence of the thick conglomerates (T<sub>1</sub>b<sub>1</sub>) in the basin, but whether these originated at the present-day

border fault or one farther west is unknown. The fact that the conglomerates are tilted and faulted means that movement on the present border fault continued after their deposition and lithification; to the south, tilted and faulted Jurassic formations indicate that faulting continued after all sedimentation had ceased in the basin (Froelich and others, 1982).

#### JOINTS IN THE CULPEPER BASIN

Lee (1979 and this report) made extensive measurements of joint surfaces in the Triassic sedimentary rocks of the Culpeper basin as shown on plate 1. A stereonet plot shows them to be mostly steeply dipping but having a wide range of azimuths (fig. 15). Despite the apparent randomness of plotted joint orientations, however, consistent north-northeast and west-northwest trends in joints in carbonate conglomerate (T<sub>1</sub>b<sub>1</sub>) are indirectly evidenced by aligned sinkholes (pl. 1), which are probably largely joint controlled.

As discussed above, there is much overlap and scatter in orientation between joints in the Culpeper basin and those in the Blue Ridge anticlinorium (figs. 14A, 15). A study by Hardcastle (1993) of more than 4,800 joints in the basin and adjacent crystalline rocks found a number of distinct trends shared by both regions (N. 13° W., N. 12° E., N. 77° E.) and one trend (N. 67° W.) largely restricted to Blue Ridge rocks. This joint pattern was not observed in the present report, perhaps due to the comparatively small number of joints measured.

#### SURFICIAL GEOLOGY

The post-Mesozoic geology of the map area is shown on plate 1. A detailed discussion of the processes active during this period and their chronology is beyond the scope of this report, but a regional map and discussion of engineering properties was provided by Froelich (1985). The materials shown include mountain slope colluvium (QTc), river terrace deposits (QTt), and flood-plain alluvium (Qal). The principle source of the colluvium is Catoctin Mountain, and the chief source for the terrace deposits and Potomac River alluvium is the upstream drainage area of the Potomac River. Alluvium derived from local sources is also found along most streams. Although the alluvium is Holocene in age, some of the colluvium and terrace deposits may be Pleistocene or older. The surficial deposits are unconformable on older units. In addition to the mappable surficial deposits, thick residual soils and saprolite mantle most of the upland bedrock surfaces, such as the areas shown as undifferentiated basement (Middle Proterozoic gneiss and late Proterozoic dikes) on plate 1. Some of the saprolite and residuum and their regional distribution in the Culpeper basin are shown in Froelich (1985).

Colluvium (QT<sub>c</sub>) occurs as bedrock clasts embedded in gravel, sand, and clayey silt in sheetlike to lensoid aprons flanking Catoctin Mountain. It is composed chiefly of unsorted angular to subangular boulders, cobbles, and pebbles of quartzite, phyllite, greenstone, and vein quartz in a loose matrix of yellowish-orange to reddish-brown micaceous sand and silt. Debris flows consisting of large jumbled blocks of Weverton Quartzite are locally conspicuous on the flanks of Catoctin Mountain. Thickness of colluvium ranges from a veneer at the eroded margins of the deposits to greater than 15 m at the foot of the mountains.

The terrace deposits (QT<sub>t</sub>) are gravel, sand, silt, and clay in fairly well bedded, gently sloping, graded deposits flanking the Potomac River. Terrace deposits have two modes of occurrence: (1) as incised but nearly continuous lowland benches 3 to 9 m above the adjacent modern flood plain and (2) as erosional upland remnants capping Manassas Sandstone and Balls Bluff Siltstone at elevations of 100 m in Maryland and 85 to 91 m and 100 to 110 m in Virginia. The gravel is composed mainly of rounded clasts of quartzite, vein quartz, and greenstone (including epidosite) and has rare clasts of chert, phyllite, and diabase; the matrix is chiefly yellowish-orange to yellowish-brown silty sand. Thickness ranges from a feather edge to about 10 m. As no direct age determinations were made, the lowermost of the highest terraces could be Pliocene or older.

The alluvium (Qal) is composed of sand, silt, gravel, and clay in layers underlying flood plains along most streams, as well as the broad flood plain of the Potomac River. The sediments are typically yellowish-brown, fairly well bedded, poorly to moderately well sorted, graded deposits; gravel commonly fills channels at the base of upward-fining sequences. Most gravel clasts in streams draining the Catoctin Mountain are subrounded quartzite, vein quartz, greenstone, and phyllite. Streams draining the Culpeper basin contain pebbles and cobbles of limestone, sandstone, siltstone, and, locally, diabase and hornfels. Alluvium is probably as much as 30 ft thick along the Potomac River and averages 20 ft in broad areas of the river flood plain at elevations from 190 to 220 ft; in tributary streams the deposits are at most 6 to 10 ft thick.

## ECONOMIC GEOLOGY

Marble from the Swift Run and basal Catoctin Formations and limonite from the Antietam Quartzite (quarry symbols on pl. 1) in the past have been quarried or mined in the map area, mostly in the 1800's. No mining or quarrying has occurred in these pre-Mesozoic crystalline rocks for many decades, and the resource potential is considered low.

In the Culpeper basin, potential resources include those for construction materials, agricultural lime, brick, and tile. Ground water is discussed in "Hydrogeology" below. No active quarries are present, but several

abandoned quarries were operated in the limestone conglomerate of the Leesburg Member of the Balls Bluff Siltstone northeast of Lucketts near old lime kilns along State Route 658. Early Mesozoic diabase is rare in this quadrangle, and only one small body northeast of Lucketts is potentially large enough to sustain an open-pit quarry operation. Much larger bodies of diabase are quarried nearby, and large volumes of better quality limestone are available and quarried in adjacent areas.

Although extensive deposits of alluvium, terrace gravel, and colluvium, largely composed of resistant quartzite clasts, are common in this area, none have been commercially exploited, although borrow pits for local usage and fill are known. The deposits have irregular thickness, are poorly sorted, and commonly are in designated parkland and thus are not of economic interest.

Three samples of red-brown Triassic shale and sandy siltstone in the Waterford quadrangle have been tested for firing properties (Calver and others, 1961; samples R-237, R-238, and R-240). Only sample R-238 from the lower fluvial part of the Balls Bluff Siltstone showed potential use for brick. Commercial clay deposits are currently being exploited for brick and tile from much more extensive Triassic deposits elsewhere in the Culpeper basin and apparently fill the present needs. A regional discussion of mineral resources in the Culpeper basin is provided by Froelich and Leavy (1981), and engineering and geotechnical characteristics of the bedrock in the Culpeper basin are discussed in Leavy and others (1983).

## HYDROGEOLOGY

In terms of bedrock control of surface flow and ground-water permeability, the map area consists of three regimes, each having characteristic rock properties and structural fabrics that influence local hydrology: (1) the dissected plateau west of Catoctin Mountain, (2) Catoctin Mountain and its flanks, and (3) the lowlands of the Culpeper basin. In the western plateau the obvious structural features, which may exert a considerable influence on ground-water flow, are the closely spaced, northeast-striking, moderately to steeply dipping sheetlike metadiabase dikes intruding gneiss, together with the subparallel and generally pervasive Paleozoic schistosity developed in both lithologies. This overall fabric contrasts with that of the Catoctin Mountain and the uplands along its flanks, which are underlain by relatively massive metavolcanic rocks and finely layered metasedimentary rocks, which have a generally gently dipping and broadly warped fine-grained internal fabric. In the Culpeper basin, the dominant hydrogeologic factors are the west-dipping sedimentary strata, which contain carbonate conglomerates having high dissolution potential. Superimposed on the gross structural features are local joints and faults of widely varying orien-

tations that act in concert with the regional structures to control the local hydrology. In the Culpeper basin, joint and fault trends in the carbonate conglomerates have apparently influenced the locations of aligned areas of both recharge (sinkholes) and discharge (springs or seeps). In terms of ground-water flow, the Culpeper basin is likely to be the most permeable, the Catoctin Mountain uplands the least, and the western plateau intermediate. The pre-Mesozoic crystalline rocks produce water-well yields ranging from highest to lowest in the following order: basement gneiss-dike complex, Swift Run Formation, Weverton Quartzite, Harpers Formation, and Catoctin Formation (Brutus Cooper, Loudoun County Department of Natural Resources, written commun., 1992).

In the Culpeper basin portion of the map area, ground water of good quality and in volumes more than adequate for domestic use is available at depths less than 150 m. Areas of potential ground-water recharge and discharge in the Culpeper basin are shown (pl. 1) by sinkholes and depressions (asterisks) and springs and seeps (spring symbols), respectively. The carbonate conglomerates have the highest yields of any aquifer in the Culpeper basin. In areas underlain by the Leesburg Member of the Balls Bluff Siltstone, numerous springs discharge at elevations from 240 to 260 ft (pl. 1). Hydrology of the Culpeper basin as a whole is discussed in Laczniak and Zenone (1985) and Froelich (1989).

Sinkholes and subsidence pits (asterisks, pl. 1), mapped in 1991 by Alex Blackburn (Loudoun County Department of Natural Resources, written commun., 1991), are subtle surface depressions having local relief of about 0.6 to 0.9 m. Sinkholes are developed in areas underlain by limestone conglomerate of the Leesburg Member of the Balls Bluff Siltstone or by residuum developed on it, whereas subsidence pits are developed in areas underlain mainly by colluvium, and locally terrace deposits that overlie limestone conglomerate of the Leesburg Member, assumed to be dissolved at depth. The presence of sinkholes or subsidence pits are *prima facie* evidence of past or current solution, subsidence, or collapse of soluble carbonate bedrock, mainly in areas of active migration of ground water or of recharge from infiltrating surface water. As mentioned above, the sinkholes are commonly aligned along consistent trends (north-northeast and west-northwest) that are parallel to joints mapped on surface outcrops of limestone conglomerate. Joint intersections along these trends are likely sites for fractured bedrock and zones of weakness capable of solution and enlargement by infiltrating ground water.

In contrast, springs (spring symbol, pl. 1) are zones of upward hydraulic gradient and ground-water discharge from the Leesburg Member. Other sites of discharge (spring symbol D, pl. 1) are persistent swampy or boggy areas at comparable elevations. Ground-water discharge occurs at sites where the regional potentiometric surface is locally

above ground surface, commonly in stream valleys. Tufa deposits (half-filled square, pl. 1), dry valleys, and caves and enlarged cavities (triangles, pl. 1), lie at regionally low elevations and may be surface exposures of formerly subterranean solution features.

## REFERENCES CITED

- Aleinikoff, J.N., Walter, Marianne, Lyttle, P.T., Burton, W.C., Leo, G.W., Nelson, A.E., Schindler, J.S., and Southworth, C.S., 1993, U-Pb zircon and monazite ages of Middle Proterozoic rocks, northern Blue Ridge, Virginia [abs.]: *Geological Society of America Abstracts with Programs*, v. 25, no. 2, p. 2.
- Aleinikoff, J.N., Zartman, R.E., Walter, Marianne, Rankin, D.W., Lyttle, P.T., and Burton, W.C., 1995, U-Pb ages of metarhyolites of the Catoctin and Mount Rogers Formations, central and southern Appalachians—Evidence for two pulses of Iapetan rifting: *American Journal of Science*, v. 295, no. 4, p. 428–454.
- Allen, R.M., 1963, Geology and mineral resources of Greene and Madison Counties: Virginia Division of Mineral Resources Bulletin 78, 102 p.
- Bartholomew, M.J., 1977, Geology of the Greenfield and Sherrando quadrangles, Virginia: Virginia Division of Mineral Resources Publication 4, 43 p.
- Boyer, S.E., and Mitra, Gautam, 1988, Relations between deformation of crystalline basement and sedimentary cover at the basement/cover transition zone of the Appalachian Blue Ridge province, *in* Mitra, G., and Wojtal, S., eds., *Geometry and mechanisms of Appalachian thrusting, with special reference to the Appalachians*: Geological Society of America Special Paper 222, p. 119–136.
- Burton, W.C., Aleinikoff, J.N., Southworth, C.S., and Lyttle, P.T., 1994, Grenvillian history of intrusion and deformation, northern Blue Ridge, Virginia [abs.]: *Geological Society of America Abstracts with Programs*, v. 26, no. 4, p. 5.
- Burton, W.C., Froelich, A.J., Schindler, J.S., and Southworth, C.S., 1992b, Geologic map of Loudoun County, Virginia: U.S. Geological Survey Open-File Map 92–716, scale 1:100,000.
- Burton, W.C., Kunk, M.J., and Lyttle, P.T., 1992a, Age constraints on the timing of regional cleavage formation in the Blue Ridge anticlinorium, northernmost Virginia [abs.]: *Geological Society of America Abstracts with Programs*, v. 24, no. 2, p. 5.
- Burton, W.C., and Southworth, C.S., 1993, Garnet-graphite paragneiss and other country rocks in granitic Grenvillian basement, Blue Ridge anticlinorium, northern Virginia and Maryland [abs.]: *Geological Society of America Abstracts with Programs*, v. 25, no. 4, p. 6.
- Calver, J.L., Hamlin, H.P., and Wood, R.S., 1961, Analyses of clay, shale, and related materials—Northern counties: Virginia Division of Mineral Resources, Mineral Resources Report 2, 194 p.
- Cloos, Ernst, 1941, Geologic map of Washington County: Maryland Geological Survey, scale 1:62,500.
- , 1947, Oolite deformation in the South Mountain fold, Maryland: *Geological Society of America Bulletin*, v. 58, no. 9, p. 843–918.

- Cornet, Bruce, 1977, The palynostratigraphy and age of the Newark Supergroup: University Park, Pennsylvania State University, Ph.D. thesis, 504 p.
- Drake, A.A., 1984, The Reading Prong of New Jersey and eastern Pennsylvania—An appraisal of rock relations and chemistry of a major Proterozoic terrane in the Appalachians, *in* Bartholomew, M.J., ed., The Grenville event in the Appalachians and related topics: Geological Society of America Special Paper 194, p. 75–108.
- Evenshade, G.H., 1986, Geology of the Marshall quadrangle, Fauquier County, Virginia: U.S. Geological Survey Bulletin 1560, 60 p.
- Evans, M.A., 1989, The structural geometry and evolution of foreland thrust systems, northern Virginia: Geological Society of America Bulletin, v. 101, p. 339–354.
- Fauth, J.L., and Brezinski, D.K., 1994, Geologic map of the Middletown quadrangle, Frederick and Washington Counties, Maryland: Baltimore, Maryland Geological Survey, scale 1:24,000, 1 sheet.
- Froelich, A.J., 1985, Map and geotechnical properties of surface materials of the Culpeper basin and vicinity, Virginia and Maryland: U.S. Geological Survey Miscellaneous Investigations Series Map I-1313-E, scale 1:125,000.
- 1989, Maps showing geologic and hydrologic factors affecting land-use planning in the Culpeper basin, Virginia and Maryland: U.S. Geological Survey Miscellaneous Investigations Series Map I-1313-J, scale 1:125,000.
- Froelich, A.J., and Leavy, B.D., 1981, Mineral resources map of the Culpeper basin, Virginia and Maryland: U.S. Geological Survey Miscellaneous Investigations Series Map I-1313-B, scale 1:125,000.
- Froelich, A.J., Leavy, B.D., and Lindholm, R.C., 1982, Geologic traverse across the Culpeper basin (Triassic-Jurassic) of northern Virginia, *in* Lyttle, P.T., ed., Central Appalachian geology, Northeast–Southeast Section of the Geological Society of America Field Trip Guidebooks, field trip 3: Falls Church, Va., American Geological Institute, p. 55–81.
- Furcron, A.S., 1939, Geology and mineral resources of the Warrenton quadrangle, Virginia: Virginia Geological Survey Bulletin 54, 94 p.
- Gates, A.E., Simpson, Carol, and Glover, Lynn, III, 1986, Appalachian Carboniferous strike-slip faults—An example from Brookneal, Virginia: *Tectonics*, v. 5, p. 119–133.
- Hardcastle, Ken, 1993, Fracture fabric of the Mesozoic Culpeper basin and adjacent, pre-Triassic crystalline basement rocks [abs.]: Geological Society of America Abstracts with Programs, v. 25, no. 2, p. 21.
- Harris, L.D., 1979, Similarities between the thick-skinned Blue Ridge anticlinorium and the thin-skinned Powell Valley anticline: Geological Society of America Bulletin, pt. 1, v. 90, p. 525–539.
- Hazlett, J.M., 1978, Petrology and provenance of the Triassic limestone conglomerate in the vicinity of Leesburg, Virginia: Washington, D.C., The George Washington University, M.S. thesis, 100 p.
- Herz, Norman, and Force, E.R., 1984, Rock suites in Grenvillian terrane of the Roseland district, Virginia, *in* Bartholomew, M.J., ed., The Grenville event in the Appalachians and related topics: Geological Society of America Special Paper 194, p. 187–214.
- Hillhouse, D.N., 1960, Geology of the Piney River-Roseland titanium area, Nelson and Amherst Counties, Virginia: Blacksburg, Virginia Polytechnical Institute and State University, Ph.D. dissertation, 129 p.
- Holden, R.J., 1907, Iron, *in* Watson, T.L., ed., Mineral resources of Virginia: Lynchburg, Va., J.P. Bell Co., p. 402–491.
- Howard, J.L., 1991, Lithofacies of the Precambrian basement complex in the northernmost Blue Ridge province of Virginia: *Southeastern Geology*, v. 31, no. 4, p. 191–202.
- Jonas, A.I., and Stose, G.W., 1938, Geologic map of Frederick County and adjacent parts of Washington and Carroll Counties: Maryland Geological Survey, scale 1:62,500.
- Keith, Arthur, 1894, Geology of the Catoctin Belt: U.S. Geological Survey Annual Report, no. 14, p. 285–395.
- Klein, S.W., Lyttle, P.T., and Froelich, A.J., 1990, Geologic map of the Loudoun County portion of the Middleburg quadrangle, Virginia: U.S. Geological Survey Open-File Report 90–641, scale 1:24,000.
- Klein, S.W., Lyttle, P.T., and Schindler, J.S., 1991, Late Proterozoic sedimentation and tectonics in northern Virginia, *in* Schultz, Arthur, and Compton-Gooding, Ellen, eds., Geologic evolution of the eastern United States, Northeast–Southeast Section of the Geological Society of America Field Trip Guidebook, no. 2: Virginia Museum of Natural History, p. 263–294.
- Kunk, M.J., Froelich, A.J., and Gottfried, David, 1992, Timing of emplacement of diabase dikes and sheets in the Culpeper basin and vicinity, Virginia and Maryland— $^{40}\text{Ar}/^{39}\text{Ar}$  age spectrum results from hornblende and K-feldspar in granophyres [abs.]: Geological Society of America Abstracts with Programs, v. 24, no. 2, p. 25.
- Kunk, M.J., Lyttle, P.T., Schindler, J.S., and Burton, W.C., 1993, Constraints on the thermal history of the Blue Ridge in northernmost Virginia— $^{40}\text{Ar}/^{39}\text{Ar}$  age dating results [abs.]: Geological Society of America Abstracts with Programs, v. 25, no. 2, p. 31.
- Laczniak, R.J., and Zenone, Chester, 1985, Ground-water resources of the Culpeper basin, Virginia and Maryland: U.S. Geological Survey Miscellaneous Investigations Series Map I-1313-F, scale 1:125,000.
- Leavy, B.D., 1984, Map showing planar and linear features in the Culpeper basin and vicinity, Virginia and Maryland: U.S. Geological Survey Miscellaneous Investigations Series Map I-1313-G, scale 1:125,000.
- Leavy, B.D., Froelich, A.J., and Abram, E.C., 1983, Bedrock map and geotechnical properties of rocks of the Culpeper basin and vicinity, Virginia and Maryland: U.S. Geological Survey Miscellaneous Investigation Series Map I-1313-C, scale 1:125,000.
- Lee, K.Y., 1977, Triassic stratigraphy in the northern part of the Culpeper basin, Virginia and Maryland: U.S. Geological Survey Bulletin 1422-C, 17 p.
- 1979, Geology of the Culpeper basin in the Waterford quadrangle, Loudoun County, Va.—Montgomery County, Md., *in* Triassic–Jurassic geology of the northern part of the Culpeper basin, Virginia and Maryland: U.S. Geological Survey Open-File Report 79–1557 (parts of 16 quadrangles, scale 1:24,000), 19 p.
- 1982, Thermal metamorphism of Triassic and Jurassic sedimentary rocks in the Culpeper basin, Virginia [abs.]: Geo-

- logical Society of America Abstracts with Programs, v. 14, no. 1–2, p. 34.
- Lee, K.Y., and Froelich, A.J., 1989, Triassic-Jurassic stratigraphy of the Culpeper and Barbourville basins, Virginia and Maryland: U.S. Geological Survey Professional Paper 1472, 52 p.
- Lindholm, R.C., 1979, Geologic history and stratigraphy of the Triassic-Jurassic Culpeper basin, Virginia: Geological Society of America Bulletin, pt. 2, v. 90, p. 1702–1736.
- Lindholm, R.C., Hazlett, J.M., and Fagin, S.W., 1979, Petrology of Triassic-Jurassic conglomerates in the Culpeper basin, Virginia: Journal of Sedimentary Petrology, v. 49, no. 4, p. 1245–1262.
- Lukert, M.T., and Nuckols, E.B., III, 1976, Geology of the Linden and Flint Hill quadrangles, Virginia: Virginia Division of Mineral Resources Report of Investigations 44, 83 p.
- McBirney, A.R., 1984, Igneous petrology: San Francisco, Freeman, Cooper, and Co., 509 p.
- McClelland, J., and Chiarenzelli, J., 1990, Geochronological studies in the Adirondack Mountains and implications of a Middle Proterozoic tonalitic suite, in Gower, C., Rivers, T., and Ryan, B., eds., Mid-Proterozoic geology of the southern margins of proto-Laurentia–Baltica: Geological Association of Canada Special Paper 38, p. 175–194.
- Mitra, Gautam, 1979, Ductile deformation zones in Blue Ridge basement rocks and estimation of finite strains: Geological Society of American Bulletin, pt. 1, v. 90, p. 935–951.
- Mitra, Gautam, and Elliott, David, 1980, Deformation of basement in the Blue Ridge and the development of the South Mountain cleavage, in Wones, D.R., ed., The Caledonides in the USA; Proceedings, International Geological Correlation Program Project 27—Caledonide Orogen, Blacksburg, Va., 1979: Virginia Polytechnic Institute and State University Department of Geological Sciences Memoir 2, p. 307–311.
- Mitra, Gautam, and Lukert, M.T., 1982, Geology of the Catoctin-Blue Ridge anticlinorium in northern Virginia, in Lyttle, P.T., ed., Central Appalachian geology, Northeast–Southeast Section of the Geological Society of America Field Trip Guidebooks, field trip 4: Falls Church, Va., American Geological Institute, p. 83–108.
- Moore, J.M., and Thompson, P.H., 1980, The Flinton Group—A late Precambrian metasedimentary succession in the Grenville province of eastern Ontario: Canadian Journal of Earth Sciences, v. 17, p. 1685–1707.
- Nickelsen, R.P., 1956, Geology of the Blue Ridge near Harpers Ferry, West Virginia: Geological Society of America Bulletin, v. 67, no. 3, p. 239–269.
- Nunan, W.E., 1979, Stratigraphy of the Weverton Formation, northern Blue Ridge anticlinorium: Chapel Hill, University of North Carolina, Ph.D. thesis, 215 p.
- Rankin, D.W., 1975, The continental margin of eastern North America in the southern Appalachians—The opening and closing of the proto-Atlantic Ocean: American Journal of Science, v. 275–A, p. 298–336.
- Ratcliffe, N.M., Aleinikoff, J.N., Burton, W.C., and Karabinos, P., 1991, Trondhjemitic, 1.35–1.31 Ga gneisses of the Mount Holly Complex of Vermont—Evidence for an Elzevirian event in the Grenville basement of the U.S. Appalachians: Canadian Journal of Earth Sciences, v. 28, p. 77–93.
- Reed, J.C., Jr., 1955, Catoctin Formation near Luray, Virginia: Geological Society of America Bulletin, v. 66, no. 7, p. 871–896.
- Reed, J.C., Jr., and Morgan, B.A., 1971, Chemical alteration and spilitization of Catoctin greenstones, Shenandoah National Park, Virginia: Journal of Geology, v. 79, no. 5, p. 526–548.
- Reinhardt, J., 1974, Stratigraphy, sedimentology, and Cambro-Ordovician paleogeography of the Frederick Valley, Maryland: Maryland Geological Survey Report of Investigations 23, 12 p.
- Roberts, J.K., 1923, Triassic basins of northern Virginia: The Pan-American Geologist, v. 39, no. 3, p. 185–200.
- Sinha, A.K., and Bartholomew, M.J., 1984, Evolution of the Grenville terrane in the central Virginia Appalachians, in Bartholomew, M.J., ed., The Grenville event in the Appalachians and related topics: Geological Society of America Special Paper 194, p. 175–186.
- Smoot, J.P., 1991, Sedimentary facies and depositional environments of early Mesozoic Newark Supergroup basins, eastern North America—Palaeogeography, palaeoclimatology, palaeoecology: Amsterdam, Elsevier Science Publishers, v. 84, p. 369–423.
- Southworth, C.S., 1991, Geologic map of the Loudoun County, Virginia, part of the Harpers Ferry quadrangle: U.S. Geological Survey Miscellaneous Field Studies Map MF-2173, scale 1:24,000.
- Stose, A.J., and Stose, G.W., 1946, Geology of Carroll and Frederick Counties, in The physical features of Carroll County and Frederick County: State of Maryland Department of Geology, Mines, and Water Resources, p. 11–131.
- Sutter, J.F., 1985, Progress on geochronology of Mesozoic diabase and basalts, in Proceedings of the Second U.S. Geological Survey Workshop on the early Mesozoic basins of the eastern United States: U.S. Geological Survey Circular 946, p. 10–114.
- 1988, Innovative approaches to the dating of igneous events in the early Mesozoic basins of the eastern United States, in Froelich, A.J., and Robinson, G.R., Jr., Studies of the early Mesozoic basins of the eastern United States: U.S. Geological Survey Bulletin 1776, p. 194–200.
- Weigand, P.W., and Ragland, P.C., 1970, Geochemistry of Mesozoic dolerite dikes from eastern North America: Contributions to Mineralogy and Petrology, v. 29, no. 3, p. 195–214.
- Whittaker, J.C., 1955, Geology of Catoctin Mountain, Maryland and Virginia: Geological Society of America Bulletin, v. 66, p. 435–462.



